AD_____

Award Number: DAMD17-00-1-0577

TITLE: Biomechanical Studies and Optical Digitizer Development for Enhanced Orthopedic Footwear

PRINCIPAL INVESTIGATOR: Vern L. Houston, Ph.D., C.P. Mason, W.K. Ling, Ph.D., G. Luo, Ph.D., M.A. Garbarini, C.M. Cruise, M.D.

CONTRACTING ORGANIZATION: East River Research Corporation of New York
New York, New York 10010

REPORT DATE: September 2001

TYPE OF REPORT: Annual

PREPARED FOR: U.S. Army Medical Research and Materiel Command
Fort Detrick, Maryland 21702-5012

DISTRIBUTION STATEMENT: Approved for Public Release;
Distribution Unlimited

20020124 239

REPORT DOCUMENTATION PAGE

1. AGENCY USE ONLY (Leave blank)	2. REPORT DATE September 2001	3. REPORT TYPE AND DATES COVERED Annual (15 Aug 00 – 15 Aug 01)

4. TITLE AND SUBTITLE
Biomechanical Studies and Optical Digitizer Development for Enhanced Orthopedic Footwear

5. FUNDING NUMBERS
DAMD17-00-1-0577

6. AUTHOR(S)
Vern L. Houston, Ph.D., C.P. Mason, W.K. Ling, Ph.D., G. Luo, Ph.D., M.A. Garbarini, C.M. Cruise, M.D.

7. PERFORMING ORGANIZATION NAME(S) AND ADDRESS(ES)

East River Research Corporation of New York
New York, New York 10010

E-Mail: vlh3@nyu.edu

8. PERFORMING ORGANIZATION REPORT NUMBER

9. SPONSORING / MONITORING AGENCY NAME(S) AND ADDRESS(ES)

U.S. Army Medical Research and Materiel Command
Fort Detrick, Maryland 21702-5012

10. SPONSORING / MONITORING AGENCY REPORT NUMBER

11. SUPPLEMENTARY NOTES
Report contains color

12a. DISTRIBUTION / AVAILABILITY STATEMENT
Approved for Public Release; Distribution Unlimited

12b. DISTRIBUTION CODE

13. ABSTRACT (Maximum 200 Words)
Properly fitting, functional footwear is paramount for preventing foot/ankle discomfort and injury, and maintaining mobility of military personnel and veterans. Custom designed and manufactured orthopedic footwear is also an essential component in treatment and rehabilitative care of persons with neuromusculoskeletal foot/ankle pathologies, biomechanical disorders and injuries, and systemic disorders, such as Diabetes Mellitus and peripheral vascular disease, that secondarily affect peoples' feet/ankles. Pedorthic design is still based almost exclusively on pedorthists' subjective judgements, however, so the degree of fit and function attained and quality of footwear produced are highly dependent upon the level of training, experience, and skill of the pedorthist. The objective of this project is to develop quantitative methods for effective, expeditious, repeatable, and consistent design and manufacture of well-fitting, comfortable, and functional orthopedic footwear. To accomplish this a 3-D optical digitizer is being developed capable of rapidly and accurately scanning peoples' feet/ankles in natural and prescribed alignments, in partial and full weight bearing states, with preservation of anatomical fiduciary landmarks' spatial location; together with conduct of biomechanical studies: (i) to derive measures quantifying footwear fit; (ii) to derive quantitative design specifications for orthopedic footwear components/modifications; and (iii) to determine the mechanical characteristics of insole materials.

14. Subject Terms (keywords previously assigned to proposal abstract or terms which apply to this award) Pedorthics, Foot, Shoes, Biomechanics, 3-D digitization, Computer-Aided Design and Manufacturing	15. NUMBER OF PAGES 33
	16. PRICE CODE

17. SECURITY CLASSIFICATION OF REPORT Unclassified	18. SECURITY CLASSIFICATION OF THIS PAGE Unclassified	19. SECURITY CLASSIFICATION OF ABSTRACT Unclassified	20. LIMITATION OF ABSTRACT Unlimited

Table of Contents

Introduction — Properly fitting and functional footwear is paramount for prevention of foot and ankle injuries, and is essential for maintaining mobility of military personnel, as well as that of veterans and persons in the civilian population. This is especially true for women, who have historically been plagued with foot/ankle problems from ill-fitting footwear. Studies have shown that female military personnel suffer a disproportionately high incidence (as high as 10:1) of musculoskeletal injuries during basic training compared to their male counterparts, and that a principal factor contributing to their high incidence of trauma is ill-fitting, inadequately functioning footwear [Ross and Woodward 1994; Reinker and Ozburne 1979]. Similarly, custom designed and manufactured orthopedic footwear is an essential component in the treatment and rehabilitative care of persons suffering foot/ankle biomechanical disorders and injuries, neuromusculoskeletal pathologies, and systemic disorders, such as Diabetes Mellitus, peripheral vascular disease, or arthritis, that secondarily afflict their feet and ankles [D'Ambrosia 1987; Riddle and Freeman 1988; Rodgers and Cavanagh 1989; Boulton et al. 1993; Boulton 1998; Coleman 1993; Gould 1982; Janisse 1998; Lord and Hosein 1992; Moncur and Shields 1983; Schaff and Cavanagh 1990; Tovey and Moss 1987; Wosk and Voloshin 1985; Mueller 1999; van Schie et al. 2000; Kelly, et al. 2000]. Properly fitting, functional, comfortable footwear can be the difference between independent, unaided mobility, and forced reliance on crutches, or confinement to a wheelchair for such patients, or even infliction of trauma causing ulceration, necrosis, gangrene, and consequent amputation in diabetic patients with peripheral neuropathy and vascular disease, Figure 1.

Unfortunately, design and manufacture of footwear has remained a subjective, slow, labor intensive process, highly dependent upon the level of training, experience, and skill of the pedorthist(s) involved. Use of quantitative data in design, manufacture, and assessment of fit and performance in Pedorthics is quite limited, typically involving at most a limited set of 2-D measurements (usually just heel-to-toe length and metatarsal ball width). More exacting measures of pedal 3-D geometry, tissue morphology, and biomechanical function are rarely considered. As a consequence, the fit, function, and level of comfort afforded by footwear (especially orthopedic footwear) is quite imprecise and inconsistent. It is tolerably adequate at best. Although some studies have been conducted in which foot/shoe plantar interface pressures at various locations have been recorded, the work reported has been principally limited to case reports and phenomenological explorations [Mueller, et al. 1994; Schaff 1993; Young 1993; Rose, et al. 1992; Donaghue, et al. 1996]. Few, if any, controlled, quantitative investigations have been conducted, from which general principles and quantitative specifications for design of footwear and associated orthopedic modifications and supplemental components can be derived. Such research, leading to development of improved procedures and better equipment enabling effective, efficient, expeditious, and consistent design and manufacture of well-fitting, functional, and comfortable (orthopedic) footwear for US military personnel, veterans, and civilians is needed.

The objective of this project is to develop knowledge, equipment, and techniques for quantitative design and manufacture of well-fitting, comfortable, and functional (orthopedic) footwear. Specifically, a 3-D optical digitizer is being developed that can rapidly, accurately, repeatably and consistently scan peoples' feet and ankles in natural and prescribed orthopedic alignments, in partial and full weight bearing states, registering the spatial location of fiduciary anatomical landmarks. Biomechanical studies are also being conducted: (i) to derive measures quantifying footwear fit; (ii) to derive quantitative design specifications for orthopedic footwear components

and modifications; and (iii) to characterize the mechanical properties and performance of insole materials.

Project Research

The project research has been divided into six respective constituent areas: (1) Pedorthic Optical Digitizer Development; (2) Quantification of Footwear Fit; (3) Assessment of Military Footwear/Last Fit; (4) Footwear Biomechanical Studies; (5) Footwear Material Mechanical Testing; (6) Summary Analysis and Documentation of Results. Work on the component tasks in each of these respective areas is being conducted concurrently as described below, and as delineated in the Project Statement of Work.

Pedorthic Optical Digitizer Development — Specifications and design sketches for optical scan heads, translation rails, and servo–electromechanical drive assemblies for a pedorthic optical digitizer, and an associated subject support fixture were prepared, Figure 2. Estimates were solicited, and a contract for procurement of the requisite components was negotiated. The components were received at the end of the twelfth month of the project, and assembly and testing begun. Work on development of associated software for control of the digitizer, and for optical scan signal acquisition, processing, analysis, and visualization was begun, adapting the programs created by the investigators for use with their prosthetics–orthotics optical digitizers where possible [Houston, et al. 1998a, 1995]. Work on adaptation of the automatic landmark detection, identification, and registration (ALDIR) neural network software developed by the investigators for preservation of the relative spatial locations of fiduciary anatomical landmarks from optical scan image intensity and range measurements was also begun. Scans of the feet and ankles of two experimental subjects were acquired and used in developmental testing, Figure 3. A design for an orthopedically contoured, pedal support platen, fabricated from transparent, low refractive index plastic was developed, and a prototype platen fabricated, Figure 4. Laboratory tests of the platen's transmissivity and refractivity were performed, and development of an algorithm for compensation of image refractive distortion, and for mitigation of image corruption from scan signal multiple reflections was begun, Figure 4 b and c. Development, and calibration, laboratory and clinical testing of the pedorthic digitizer will be completed in the second project year.

Quantification of Footwear Fit — To establish a reference for quantification of footwear fit, US military Lasts for female personnel footwear, and for US military oxford style shoes for male personnel, were obtained from the Defense Logistics Agency, Defense Personnel Service Center (DLA DPSC). Approximately one half (144) of these Last sets have now been digitized with the VA NYHHS Prosthetics–Orthotics Optical Digitizer, and the resulting measurement files compiled in the project computerized pedorthic database, and entered into the Last Library of the VA Pedorthics CAD/CAM System [Houston, et al. 1998b], Figure 5. Summary statistics were also tabulated from the investigators' VA RR&DS sponsored survey of the medical and pedorthic records (including orthopedic Lasts, shoe modifications and upper patterns) of 290 "representative" pedorthic patients' from the VA National Footwear Center. Analysis of the data was performed to establish pedal regions' loading tolerances, and relative susceptibility to injury, biomechanical disorders, and pathologies, Table 1. The remaining project tasks in this area — calibration, laboratory and clinical testing of a Tekscan IScan stress measurement system with custom fabricated, high sensitivity, model #6910 FVR miniature array transducers; IScan measurement of dorsal pedal/footwear interface stresses in synchrony with simultaneous FScan measurement of pedal plantar pressures in "well-fitting," and in "ill-fitting," military footwear

during stance and gait for twelve test subjects — are targeted for completion in the second project year, as detailed in the Project Statement of Work.

Assessment of Military Footwear Last Fit — As noted in the previous section, two sets of military footwear Lasts were obtained from the DLA DPSC, approximately half of which have now been digitized, and the resulting measurement files entered into the project pedorthic database, and into the VA Pedorthics CAD System Last Library. In addition, thirty-five normal, healthy subjects of military service age have been recruited, and casts and scans, together with a set of 23 manual measurements, have been acquired of their feet and ankles, Table 2. (The parametric measures acquired correspond to the principal pedal measurements recorded in the comprehensive military personnel lower limb anthropometric survey of Parham, et al. These measures are being acquired as a control to ensure the subjects sampled in the project are "representative" of the US Military population.) Comparative analysis of the resulting data to identify the regions that evidence conformance, and those that exhibit non-compliance, between the subjects' feet/ankles and the respective Lasts (and by extension the corresponding footwear that would be issued to the subjects under current military practice), Figure 6. Work in this research area will continue into the second project year.

Footwear Biomechanical Studies — Investigations measuring pedal/footwear interface stresses, ground reaction forces, and subject body segment kinematics in stance and gait incurred in footwear with commonly prescribed orthopedic modifications and components, were begun. In particular, laboratory testing, and trials with two subjects, were conducted to calibrate and assay synchrony of the project biomechanical test instrumentation, comprised of IScan and FScan pedal stress measurement systems, a GaitRite Electronic Walkway, a Kistler force plate, and a Qualisys 3-D Video Motion Analysis System. Studies of the effects of shoe outer sole rocker radius of curvature and fulcrum position, and of shoe outer sole forefoot and heel width on pedal/footwear interface stress magnitudes, gradients, spatial distribution and temporal durations; ground reaction force magnitudes, locations and durations; and lower limb segmental kinematics, were performed and will continue in the second project year, Figures 7 – 10.

In further biomechanical studies, the compressive creep response of the pedal plantar tissue at the heel and at the first metatarsal head of six subjects' feet were measured using the VA NYHHS servo-mechanical, force/position feedback, indentor [Houston, et al. 1998c], Figure 11. Magnetic resonance scans of two of the subjects' feet were also acquired, and the resulting images of their respective pedal tissue morphology segmented and digitized, and corresponding nonlinear finite element (FE) models developed. The pedal FE models constructed were then used to analyze the stresses and strains incurred at the heel and at the metatarsal heads under normal loading conditions, and in the presence of a vertical heel spur, as a function of pedorthic treatment with insoles with a range of material stiffnesses and design geometries, Figures 12 – 14, Tables 3 and 4. Results from these studies show maximum stresses in pedal plantar tissues occur directly underneath the calcaneus and first metatarsal head, and at or near the surface of the plantar fat pad. Maximum strains, however, occur underneath and adjacent to the calcaneus and first metatarsal head. Alteration of insole design geometry by introduction of reliefs, either removing material or by incorporation of softer secondary materials under the heel and metatarsal heads (as is common practice) was shown to only minimally affect tissue stresses and strains. Incorporation of appropriate reliefs does, however, slightly reduce associated strain energy densities in the tissues. Because of the Dunnell effect, use of non-contoured, cylindrical reliefs introduces large localized stresses, strains, and stress gradients in pedal tissues at the border of the relief. Such design geometries should, therefore, be avoided. The greatest reductions

in stress, strain, and strain energy magnitudes are achieved by custom contouring of insoles to match patients' "natural" pedal tissue contours and by extending the insole borders proximally around the fat pad to constrain its rheological displacement under load. Production of orthopedic insoles for patients with this optimal design geometry out of a viscoelastic material three to four times the stiffness of the patient's pedal plantar tissues, enables reductions as high as 50% in maximum tissue stresses and strains, and 90% in maximum strain energy densities, to be achieved, respectively, during stance. In pathologic cases with calcaneal osteophytes (heel spurs) and/or arthritic osseous deformities, with vertical components, reductions of as much as 95% in tissue stresses and strains, and 98% in strain energies densities can be attained in stance. Work in this project area refining pedal FE models and examining the effects of dynamic forces incurred during gait will continue in the second project year.

Footwear Material Mechanical Testing — Samples of the four materials most commonly used in manufacture of orthopedic insoles (i.e., polyurethane foam, polyethylene foam, silicone, and ethyl vinyl acetate foam (EVA)) were obtained. Specimens of each material in two different compositions/densities were prepared, and mechanical tests were performed in accordance with ASTM prescribed procedures, measuring the materials' respective mechanical stiffnesses in creep and stress relaxation under normal and shear loads, Figure 15. Measurement of the respective materials' load damping response, impact response, hysteresis, and plastic deformation (set) will continue in the second project year. Results from the material creep and stress relaxation response tests were used in the FEA pedal plantar tissue biomechanical loading studies described above. Sample insoles of the respective materials were also prepared and tested under static, axially applied load (approximately ¼th body weight) with one experimental subject in the VA NYHHS magnetic resonance scanner, Figures 16 and 17. The pedal–pedorthic insole MRI scan results were used to compute the values of pedal tissue strain actually incurred during static, axial loading as a function of insole stiffness and geometric design. These computations are, in turn, being used to validate and refine the project pedal FE models.

Key Research Accomplishments First Project Year

- Design specifications were established, and components procured, for a prototype 3-D Pedorthic Optical Digitizer.

- Portions of the software were developed, required for: (i) control of the digitizer; (ii) acquisition, processing, analysis, visualization, and registration of digitizer camera measurements; and (iii) for processing of digitizer measurements for automatic detection, identification, and registration of pedal fiduciary anatomical landmarks.

- 144 US military footwear Lasts were optically digitized and the resulting measurement files entered into the VA NYHHS Pedorthic CAD System Last Library, and into the project pedorthic database, together with scans and manual measurements of the feet and ankles of 35 normal, healthy test subjects of military service age, for use in quantitative assessment of military footwear fit.

- The compressive creep response of six subjects' pedal plantar tissues was measured; magnetic resonance scans of two of the subjects' feet were acquired and digitized; and the results used to create corresponding pedal finite element models. The resulting FE models were then used in studies to optimize pedorthic insole design for prevention and treatment of podalgia, and for treatment of calcaneal osteocytes.

- In further biomechanical studies, a battery of measurements were acquired for analysis of the effects of shoe outer sole rocker radius of curvature and fulcrum position, and of shoe outer sole forefoot and heel width on (i) pedal/footwear interface stress magnitudes, gradients, temporal duration, and spatial distribution; (ii) on ground reaction force magnitudes, locations and durations; and (iii) on lower limb segmental kinematics;

- The creep response and stress relaxation response (characterizing the mechanical stiffness) of four of the most commonly used pedorthic insole materials were measured; magnetic resonance scans of the feet of a test subject statically, axially loaded wearing insoles, fabricated from the respective materials in a range of design geometries, were acquired.

Reportable Outcomes First Project Year

Manuscripts & Abstracts

- Houston VL, Luo G, Mason CP, Mussman M, Garbarini MA, Beattie AC, Cruise CM, Thongpop C. "FEA Optimization of Pedorthic Insole Design for Patients with Diabetes Mellitus." **Proc. 10ᵗʰ World Congress ISPO**, Glasgow, UK, July 2001; Tho10.7.

- Houston VL, Luo G, Mason CP, Mussman M, Garbarini MA, Beattie AC, Cruise CM, Thongpop C. "FEA Optimization Of Pedorthic Treatment For Podalgia," **ASME Advances in Bioengineering**, 2001; BED-Vol. 51.

Presentations

- Houston VL, Luo G, Mason CP, Mussman M, Garbarini MA, Beattie AC, Cruise CM, Thongpop C. "FEA Optimization of Pedorthic Insole Design for Patients with Diabetes Mellitus." **Proc. 10ᵗʰ World Congress ISPO**, Glasgow, UK, July 2001.

- Houston VL. "Optimization Of Pedorthic Insole Designs". 2001 Annual Mtg Texas Orthotics and Prosthetics Association, Brownsville, TX.

Informatics

- Pedal 3-D Geometric Database established with optical scans and fiduciary manual measurements of the feet/ankles of 35 subjects of military service age.

- Optically digitized measurements of 144 US military footwear Lasts were added to the Last Library of the VA Pedorthic CAD/CAM System, and to the project pedorthic database.

Conclusions

Specifications and drawings were created, and components procured and assembled, for a pedorthic optical digitizer. Portions of the software required for control of the digitizer, and for acquisition, processing, visualization, and analysis of the digitizer measurements, with automated detection, identification, and registration of pedal fiduciary anatomical landmarks, were also prepared. 144 US military footwear Lasts were digitized, and the feet/ankles of 35 normal, healthy subjects of military service age were scanned for use in evaluation of military footwear (Last) fit. Instrumentation was assembled, calibrated, and tested for measurement of pedal/footwear static and dynamic interface stresses, ground reaction forces, and body segment kinematics for quantification of footwear fit and function. Biomechanical studies of orthopedic footwear modifications and component designs were initiated, measuring the effects of variations

in shoe outer sole and heel width, and of sole rocker curvature and fulcrum position on pedal/footwear interface stresses and body segment gait kinematics. The tissue nonlinear mechanical stiffness characteristics at the heel and first metatarsal head, together with the external and internal geometry and morphology of the feet and ankles of six subjects were measured, and finite element models of two of the subjects' feet were created. The mechanical properties of four of the most common materials used in production of pedorthic insoles were measured, and the results used together with the pedal finite element models in pedorthic insole design optimization studies for treatment and prevention of podalgia, plantar fasciitis, and calcaneal osteophytes.

The pedorthic optical digitizer, which will be laboratory and clinically tested in the second project year, will be capable of rapidly, accurately, repeatably and consistently measuring the 3-D spatial geometry and surface topography of peoples' feet and ankles, in natural and prescribed orthopedic alignments, in partial and full weight bearing states, registering the spatial location of fiduciary anatomical landmarks. As such, it will be a powerful tool, with application in numerous areas in Pedorthics, Podiatrics, and Orthopaedics. As illustrated in Figure 6, it can be used at military induction and training sites to ensure accurate and consistent issuance of appropriately fitting footwear, especially to incoming female personnel who are more susceptible to injury. In addition, as demonstrated in field trials of the VA Pedorthic CAD/CAM System, the optical digitizer is an essential component for rapid acquisition and input of precise, comprehensive measurements of pedal geometry for use in custom design and manufacture of well-fitting, comfortable and functional orthopedic footwear. In addition, in medical and podiatric applications, the digitizer will be a powerful quantitative tool, useful in diagnosing and monitoring treatment of pathologies and disorders that affect pedal geometry, such as vascular edema, tissue inflammatory response to osseous degeneration from arthritis or Charcot syndrome, or neuromusculoskeletal deformity resulting from chronic diabetes and arthritis. The digitizer can also be used in anthropometric surveys, compiling measurements of the pedal geometry of a statistically significant and powerful sample of persons of military service age, for use in design of new, more anatomically shaped Lasts for production of better fitting, more functional, and more comfortable footwear.

Clinical use of the digitizer, providing rapid, accurate measurement of pedal geometry, coupled with knowledge acquired from biomechanical studies of pedal tissue mechanical characteristics, and pedorthic material properties, can lead to development of new, more accurate and comprehensive metrics of footwear fit, that will prevent pedal trauma, and contribute to increasing mobility and performance of military personnel, veterans, and civilian pedorthics patients. Quantitative characterization of pedal tissue and pedorthic material mechanical properties, together with characterization of the pedal/footwear interface stresses, ground reaction forces, and pedal/footwear kinematics produced during stance and gait, as illustrated in Figures 7, 8, 12, and 13, can lead to development of entirely new pedorthic materials and creative designs providing better fitting, more comfortable, and more functional footwear for military personnel, and also for custom orthopedic footwear for veterans and civilians with podiatric and orthopedic disorders. For example, as evident in the project pedorthic insole design studies summarized in Table 3, pedal tissue stresses and strains incurred under normal loading conditions, are not exceptionally large. Nonetheless, some people suffer podalgia and plantar fasciitis with increased repetitive activity. The pedal tissue stress and strain magnitudes do not change, only the duration of loading is increased. The one parameter seen to be appreciably different in these studies is tissue strain energy density. Strain energies from non-elastically

recovered deformation, dissipated in pedal tissues can, and undoubtedly do, disrupt tissue circulation and metabolism, causing pain and inflammation, and leading to tissue structural changes and mechanical failure. Development of new pedorthic insole and/or outer sole materials designed specifically to dissipate strain energies can alleviate this problem. New results, such as this, arising from quantitative, biomechanical pedorthic studies have the potential for significantly improving the level of function, comfort, and performance of footwear for military personnel, and thus their lives, as well as the lives of may veterans and civilians with podiatric and orthopedic pedal disorders and pathologies.

References

Boulton AJM. "Lowering the risk of neuropathy, foot ulcers, and amputations." **Diabetic Medicine**, 1998; 15 (Sup 4); S57–59.

Boulton AJM, Veves A, and Young MJ, "Etiopathogenesis and Management of Abnormal Foot Pressures," in **The Diabetic Foot,** 5th ed., Levin ME, O'Neal LW, and Bowker JH, eds., C. V. Mosby, St. Louis, MO, 1993; 234–246.

Coleman WC. "Footwear In a Management Program of Injury Prevention," in **The Diabetic Foot**, 5th ed., Levin ME, O'Neal LW, and Bowker JH, eds., C. V. Mosby, St. Louis, MO, 1993; 293–309.

D'Ambrosia RD. "Conservative Management of Metatarsal and Heel Pain in the Adult Foot," **Orthopedics**, 1987; 10: 137–142.

Donaghue VM, Sarnow MR, Giurini JM, Chrzan JS, Habershaw GM, and Veves A. "Longitudinal in-shoe foot pressure relief achieved by specially designed footwear in high risk diabetic patients," **Diabetes Res Clin Pract**, 1996; 31(1-3): 109–114.

Gould JS, "Conservative Management of the Hypersensitive Foot in Rheumatoid Arthritis," **Foot & Ankle**, 1982; 2: 224–229.

Houston VL, Mason CP, Beattie AC, LaBlanc KP, Luo G, Garbarini MA, and Cruise CM, "The VA-Cyberware Prosthetics-Orthotics-Pedorthics Optical Digitizers," in **CAD/CAM Systems in Pedorthics, Prosthetics & Orthotics**, U. Boenick and E.h.M. Nader, eds., Verlag Orthopadie-Technik, Berlin, Germany, 1998a; 133–163.

Houston VL, Mason CP, Luo G, Mussman M, LaBlanc KP, Beattie AC, Garbarini MA, and Cruise C. M. "An Overview of the VA Pedorthic CAD/CAM System," in **CAD/CAM Systems in Pedorthics, Prosthetics & Orthotics**, U. Boenick and E.h.M. Nader, eds., Verlag Orthopadie-Technik, Berlin, Germany, 1998b; 337–348.

Houston VL, Luo G, Mason CP, Arena L, Beattie AC, LaBlanc KP, Garbarini MA. "FEA for Quantification of Prosthetic/Orthotic/Pedorthic CAD," **CAD/CAM Systems in Pedorthics, Prosthetics & Orthotics**, U. Boenick and E.h.M. Nader, eds., Verlag Orthopadie-Technik, Berlin, Germany, 1998c; 254–276.

Houston VL, Mason CP, Beattie AC, LaBlanc KP, Garbarini MA, Lorenze EJ, and Thongpop CM. "The VA–Cyberware Optical Laser Digitizer," **J. Rehab. Res. & Devel.**, 1995 (February); 32(1): 55–73.

Janisse DJ. "Prescription footwear for arthritis of the foot and ankle," **Clin Orthop**, 1998; 349:100–107.

Janisse, DJ. "Pedorthic Care of the Diabetic Foot," in **The Diabetic Foot,** 5th ed., Levin ME, O'Neal LW, and Bowker JH, eds., C. V. Mosby, St. Louis, MO, 1993; 549–576.

Kelly VE, Mueller MJ, Sinacore DR. "Timing of peak plantar pressure during stance phase of walking." **J Amer Podiatric Med Assoc**, 2000 (Jan); 90 (1): 18–23.

Lord M, and Hosein R. "Pressure Redistribution By Moulded Inserts," **Proc. 7th World Congress ISPO, Chicago, IL, June 1992**; 279.

Moncur C, and Shields MN. "Clinical Management of Metatarsalgia in the Patient With Arthritis," **Clinical Management in Physical Therapy**, 1983; 3(4): 7–13.

Mueller MJ. "Application of plantar pressure assessment in footwear and insert design." **J Orthopaedic & Sports Physical Therapy**, 1999 (Dec); 29 (12): 747–755.

Mueller MJ, Sinacore DR, Hoogstrate S, and Daly L. "Hip and Ankle Walking Stratagies: Effect on Peak Plantar Pressures and Implications for Neuropathic Ulceration," **Arch Phys Med Rehabil**, 1994; 75: 1196–1200.

Parham KR, Gordon CC, Bensel CK. "Anthropometry of the Foot & Lower Leg of US Army Soldiers," US Army Natick Res, Devel, Engr Cntr Tech Rpt. TR–92/028, Natick, MA 1992.

Reinker KA, Ozbourne S. "A Comparison of Male and Female Orthopedic Pathology In Basic Training," **Military Med.**, 1979; 144: 532–536.

Riddle DL, and Freeman DB. "Management of a Patient With Diagnosis of Bilateral Plantar Fasciitis and Achilles Tendonitis," **Physical Therapy**, 1988; 68(12): 1913–1916.

Rodgers MM, and Cavanagh PR. "Pressure Distribution in Morton's Foot Structure," **Med. & Sci. in Sports & Exercise**, 1989; 21(1): 23–28.

Rose NE, Feiwell LA, and Cracchiolo A. "A Method for Measuring Foot Pressures Using a High Resolution, Computerized Insole Sensor: The Effect of Heel Wedges on Plantar Pressure Distribution and Center of Force," **Foot & Ankle**, 1992; 13(5): 263–271.

Ross J, Woodward A. "Risk Factors For Injury During Basic Military Training," **J. Occup. Med.**, 1994; 36: 1120–1126.

Schaff PS. "An Overview of Foot Pressure Measurement Systems," **Clin Podiatric Med Surg**, 1993; 10(3): 403–415.

Schaff PS, and Cavanagh PR. "Shoes for the Insensitive Foot: the Effect of a 'Rocker Bottom' Shoe Modification on Plantar Pressure Distribution," **Foot & Ankle**, 1990; 11(3): 129–140.

Tovey FI, and Moss MJ. "Specialist Shoes for the Diabetic Foot," in **The Foot in Diabetes**, Connor H, Boulton AJM, and Ward JD, eds., Wiley & Sons, New York, NY, 1987; 97–108.

van Schie C, Ulbrecht JS, Becker MB, Cavanagh PR. "Design criteria for rigid rocker shoes." **Foot Ankle Intl.**, 2000 (Oct); 21 (10): 833–844.

Wosk J, and Voloshin AS. "Low Back Pain: Conservative Treatment With Artificial Shock Absorbers," **Arch. Phys. Med. & Rehabil.**, 1985; 66: 145–148.

Young CR. "The FScan System of Foot Pressure Analysis," **Clin Podiatric Med Surg**, 1993; 10(3): 455–461.
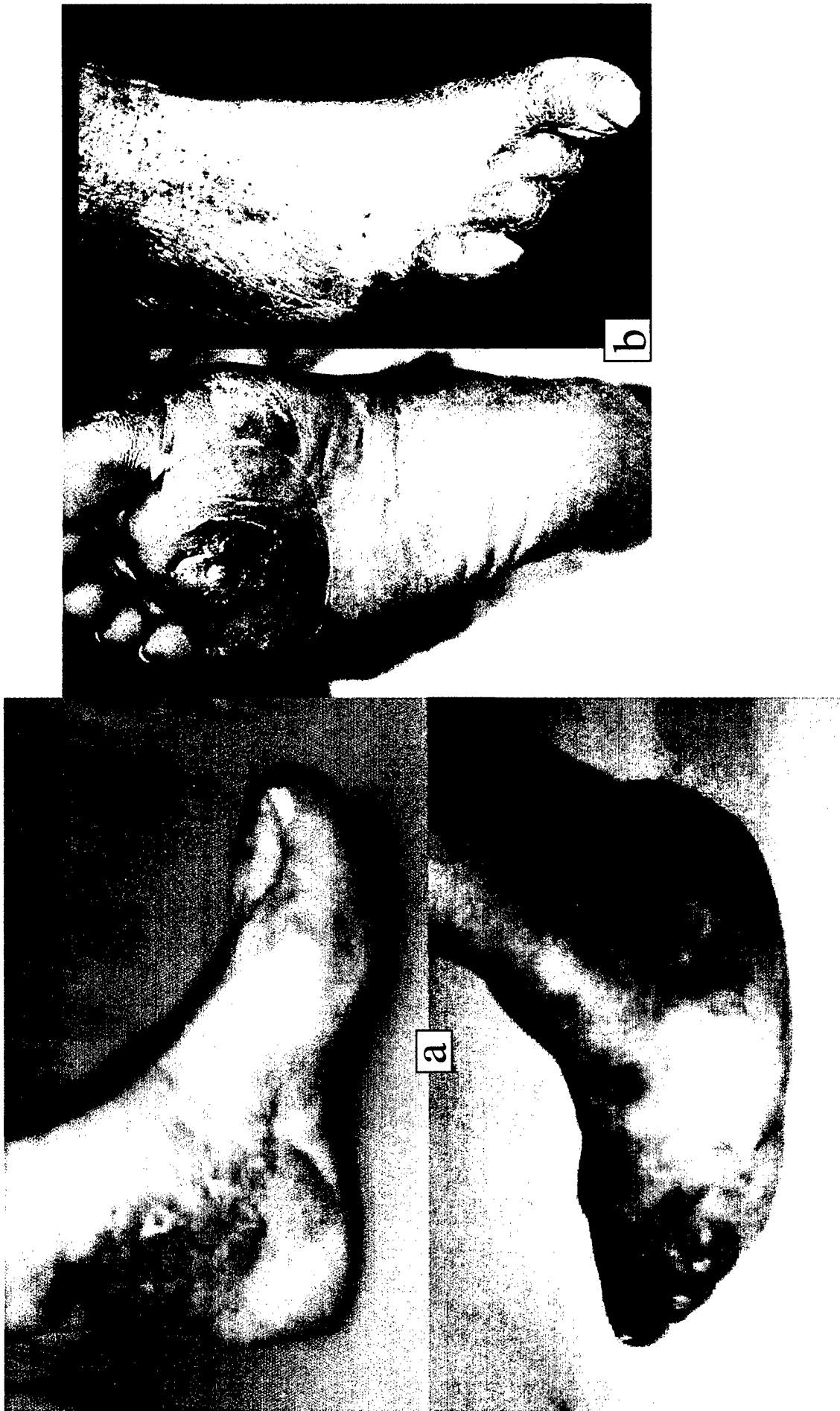
Figure 1. The feet–ankles of US Veterans requiring custom orthopedic footwear. (a) (top) Veteran with pedal shrapnel injury with consequent fused mid-foot; (bottom) paratrooper with impact injury to mid-foot; (b) Veterans with chronic Diabetic Mellitus with — (left) stage 3 decubitus ulcer under third metatarsal head; (right) resected fifth ray of forefoot from repetitive stress injury and consequent tissue necrosis and gangrene.
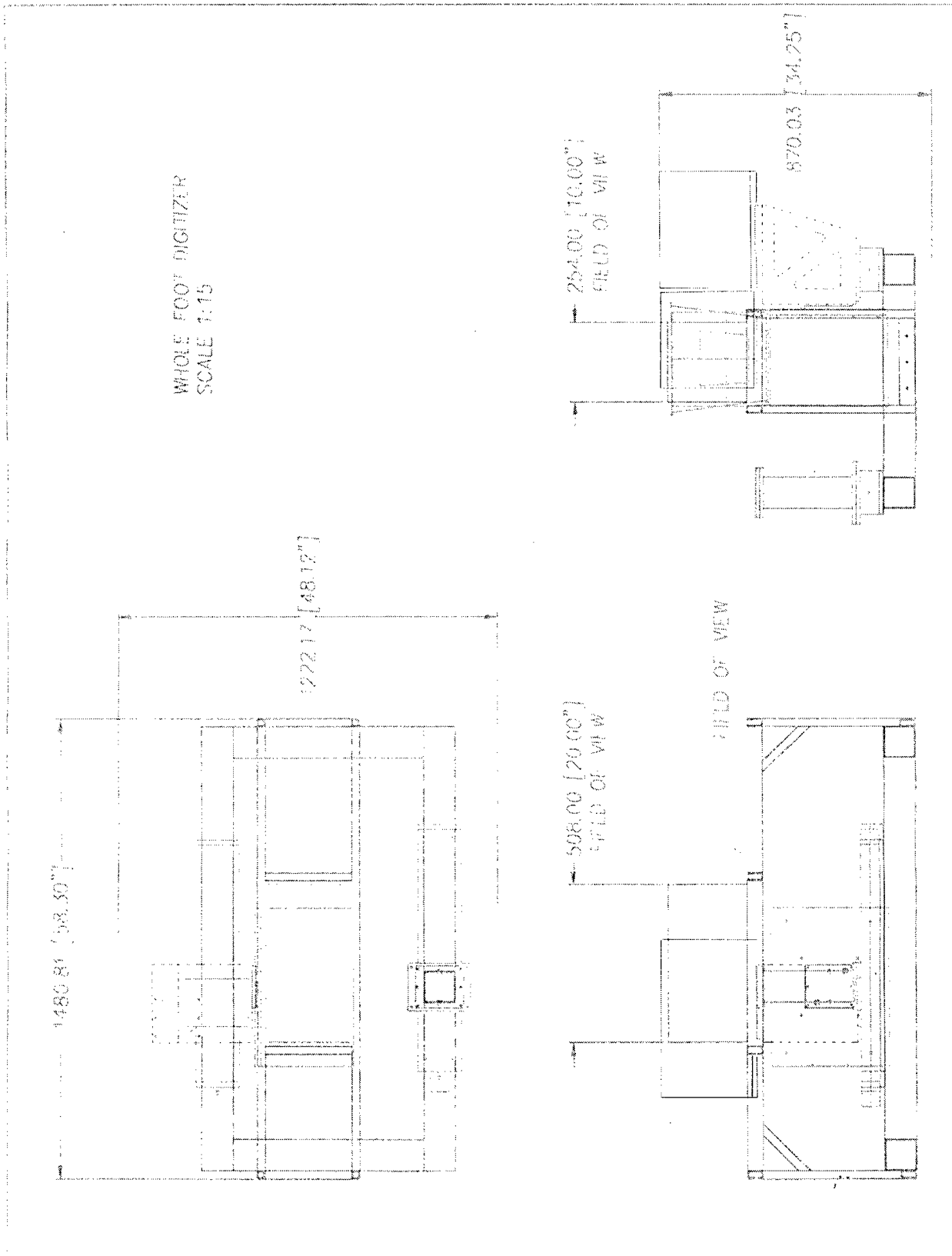
Figure 2. Design drawings for a pedorthic optical digitizer, consisting of three scan heads and servo controlled translation rails and drive assemblies. *(Prepared in collaboration with Cyberware Laboratory.)*
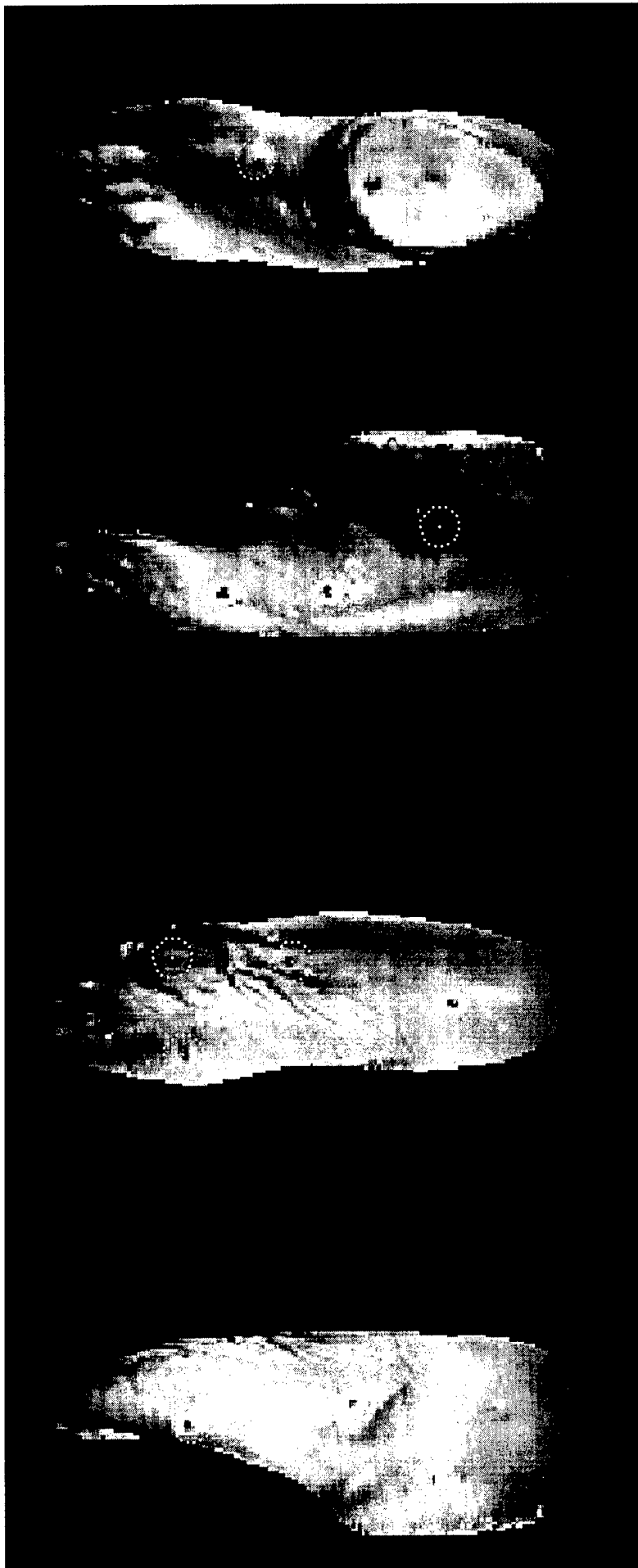
Figure 3. Output from VA NYHHS automatic landmark detection, identification, and registration (ALDIR) algorithm applied to optical digitizer camera output intensity and range measurements from the scan of a patient's foot and ankle. Dorsal and caudal views with ±42 deg offset perspectives are shown. Differences in the intensity of the laser signal reflected from the pedal surface and from the fiduciary landmarks are evident in the scan data. The encircled points are the landmarks detected by the ALDIR neural network algorithm.
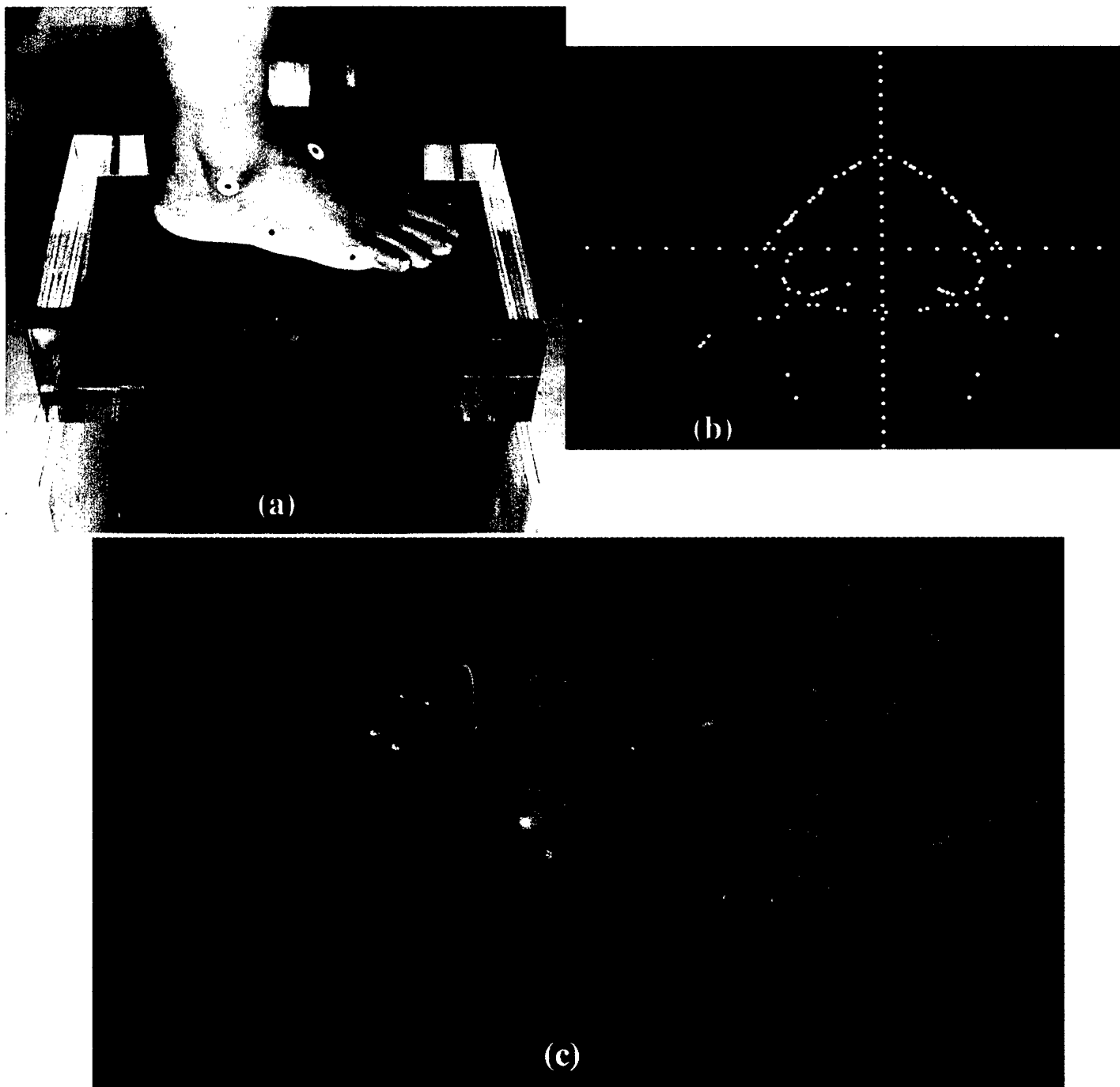
Figure 4. (a) Laboratory testing, measuring the transmissivity and refractivity of the orthopedically contoured pedal support platen, fabricated from transparent, low refractive index Lucite™. The incident near infrared source signal and multiply reflected constituent secondary and tertiary signals are visible. (b) Demonstration showing multiply reflected and refracted "noise" constituents (small red dots) of an incident source signal (large red dot); (c) Transverse cross section through the forefoot from a pedal scan illustrating corruption of the digitizer camera output signal from multiply reflected and refracted signal constituents.
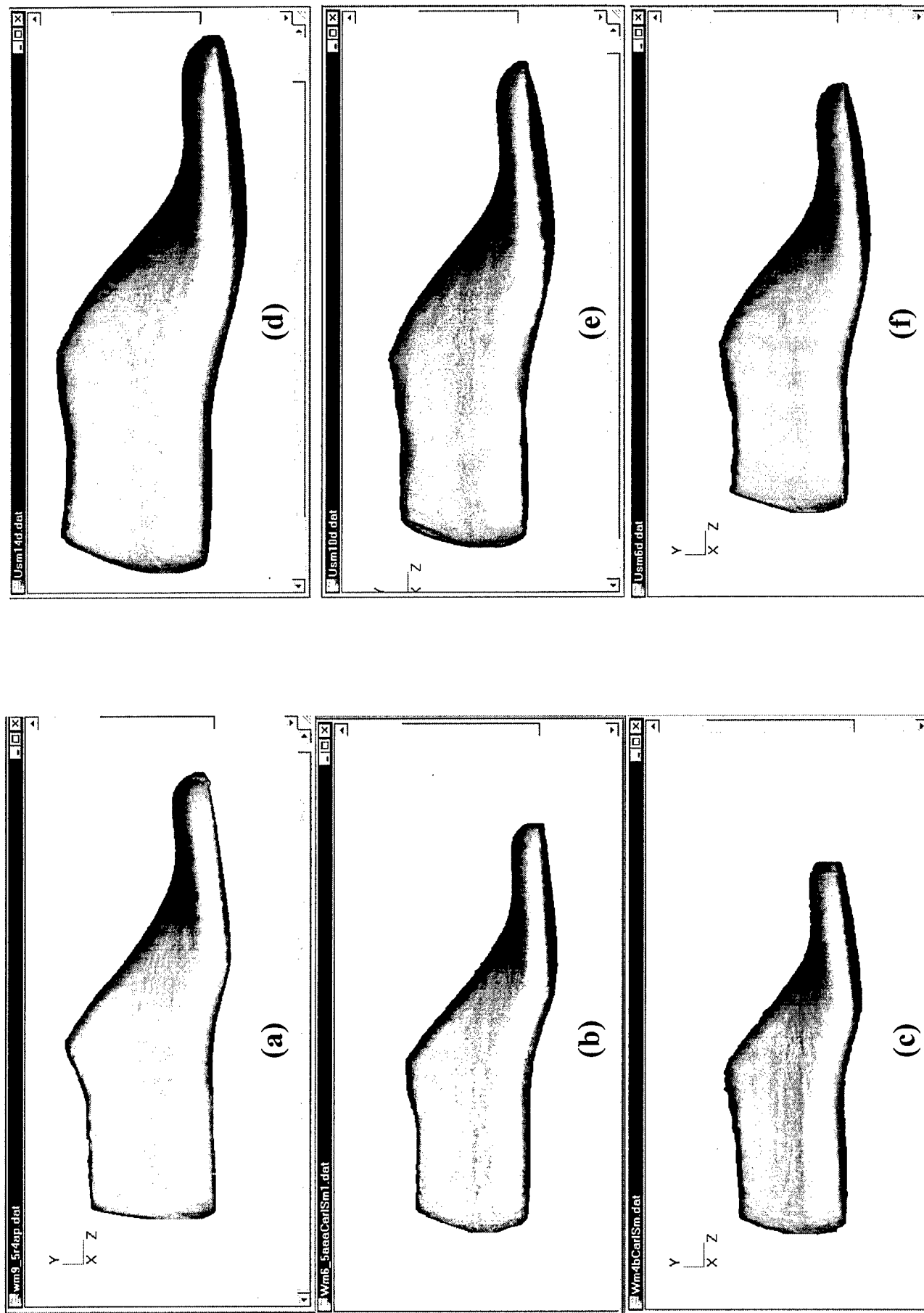
Figure 5. Shaded solid sagittal views of the DLA DPSC US Military Lasts for female personnel (a – c) and for male personnel (d – f) displayed in the VA Pedorthic CAD System. Digitized scans of the smallest, mid-size, and largest Lasts in the respective sets are shown. The algebraic (non-anatomical) scaling of the Lasts is evident.

(a)

(b)
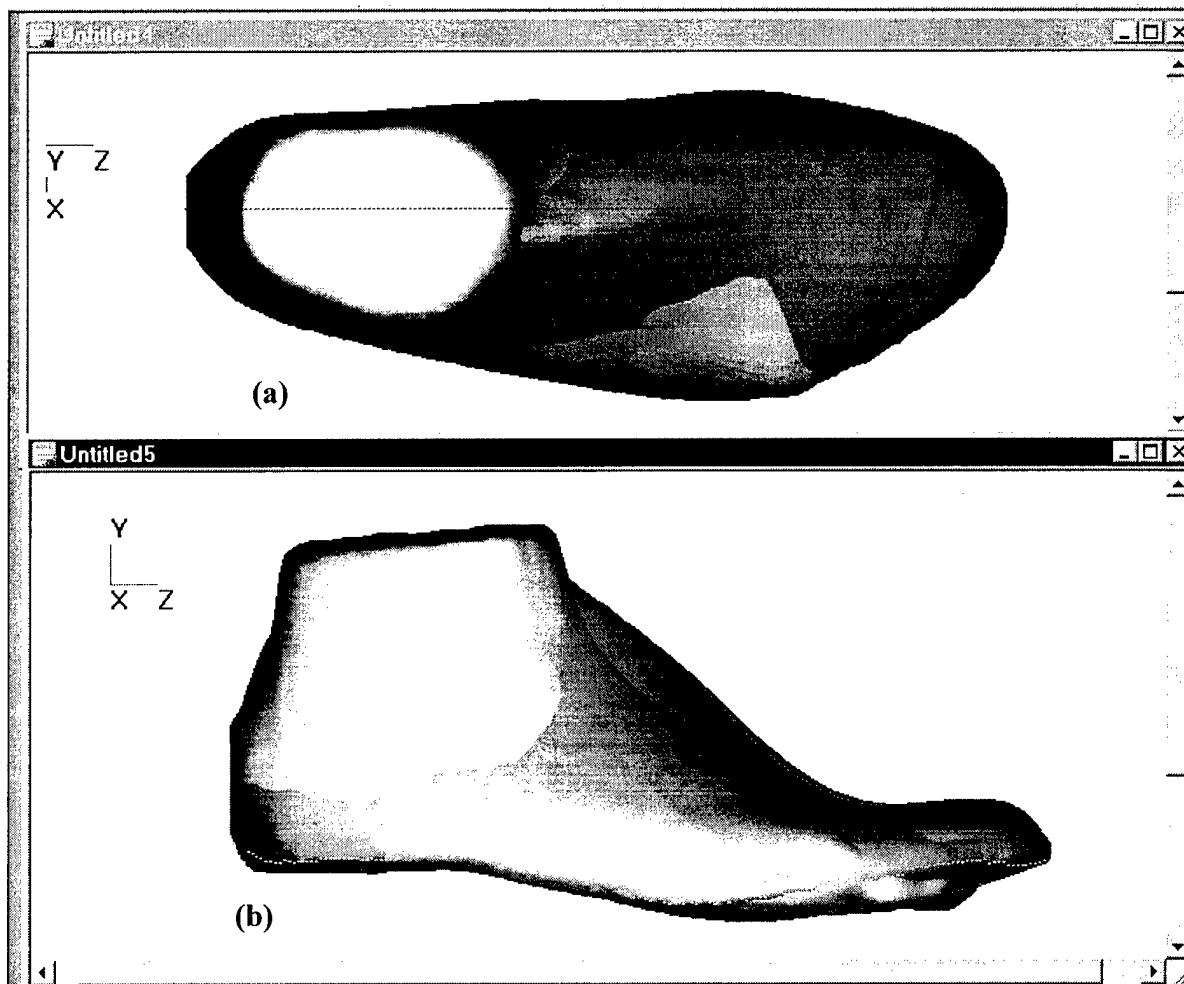
(c) Pedorthic Foot/Ankle and Footwear Last Grading Parameters

Pedorthic Grading Parameters (mm)	Parametric Dimension Test Subject Foot/Ankle	Parametric Dimension Military Footware Last	Dimensional Differences (Subj Foot/Ankle – Last)
Heel to toe length	243	254	−11
Heel to ball length	170	178	−8
Heel to crest length	108	117	−9
Ball width	95	87	+8
Heel width	69	61	+8
Span circumference	326	325	+1
Ball circumference	232	217	+15
Instep circumference	260	243	+17
Waist circumference	242	230	+12
Toe box height	23	26	−3
Total Volume (cm³)	924	670	254

Figure 6. VA Pedorthic CAD System shaded solid **(a)** dorsal and **(b)** lateral sagittal views of the foot and ankle of a normal, healthy female subject of military service age with the "best" fitting DLA DPSC US Military Last superimposed. Non-compliant regions between the subject's foot/ankle and the Last, which are at potential risk of injury, are evident. **(c)** Set of eleven pedorthic "grading" parameters, only two or three of which are typically used to assess fit, are shown for the subject's foot and the Last.
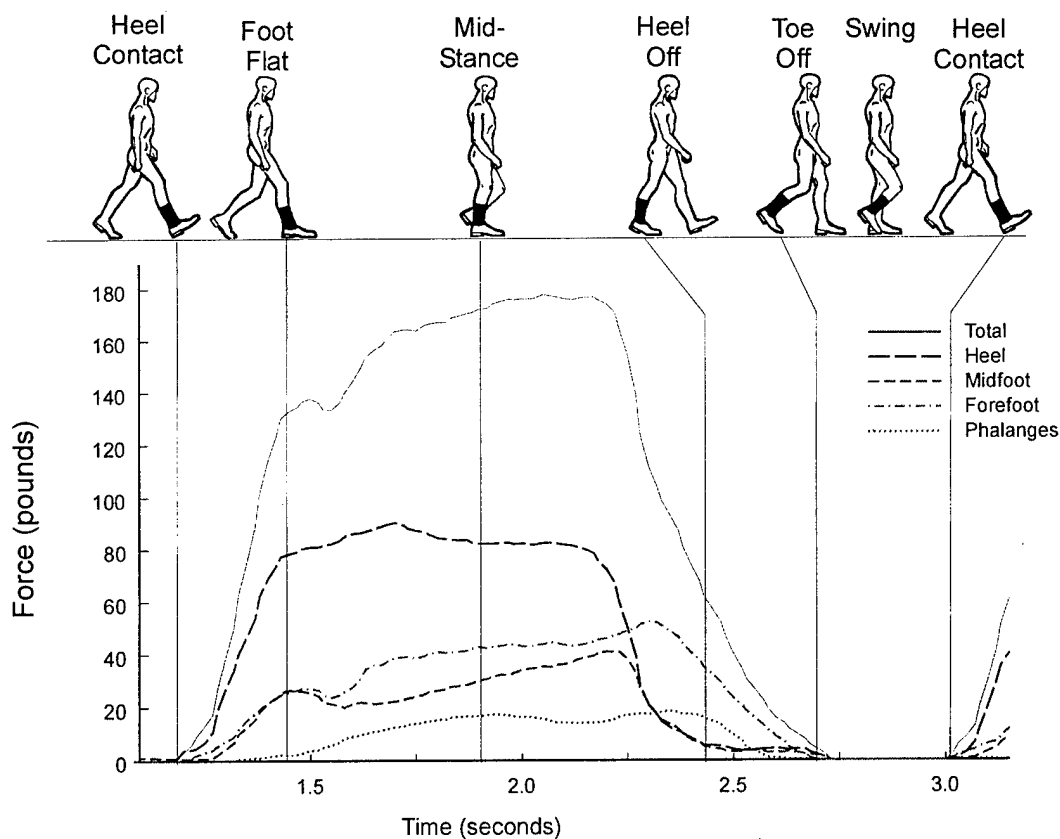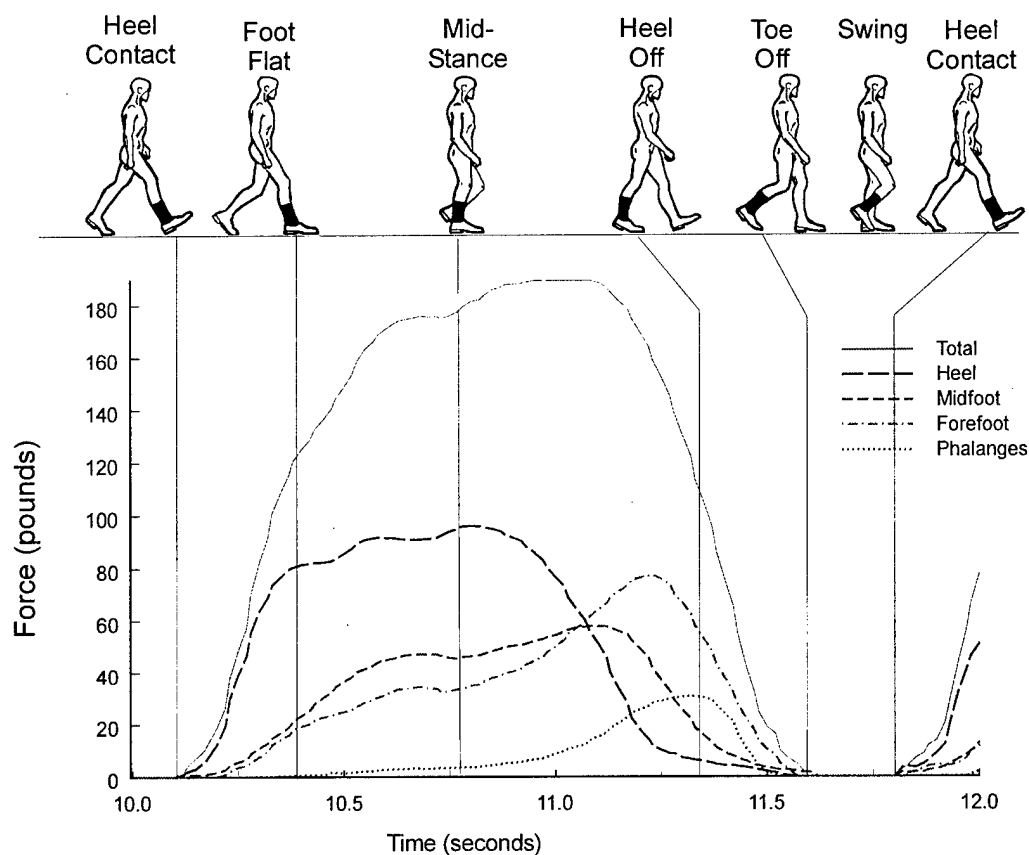
Figure 7. Footwear Biomechanical Studies showing total and regional plantar force measurements versus time from the central gait cycle in a 10 m level walking trial at user selected walking speed, for the right foot of a test subject with a neuromuscular disorder wearing oxford style shoes with: **(a)** "normal" width outer soles and heels; and **(b)** ½" extended width outer soles and heels. Non-demarcated heel contact-to-foot flat, with prolonged loading of the heel and mid-foot regions, and lengthened and reduced amplitude loading of the forefoot, indicative of a festinating gait is evident in the "normal" width sole and heel shoes. In the extended width sole and heel shoes the subject's gait is slightly improved, with heel contacttofoot flat, midstance, and heel risetotoe off gait phases being more clearly defined, and the duration of heel and midfoot loading reduced, indicating a more controlled, stabler, energy efficient gait.

(a) Normal Sole and Heel

(b) Extra Width Sole and Heel
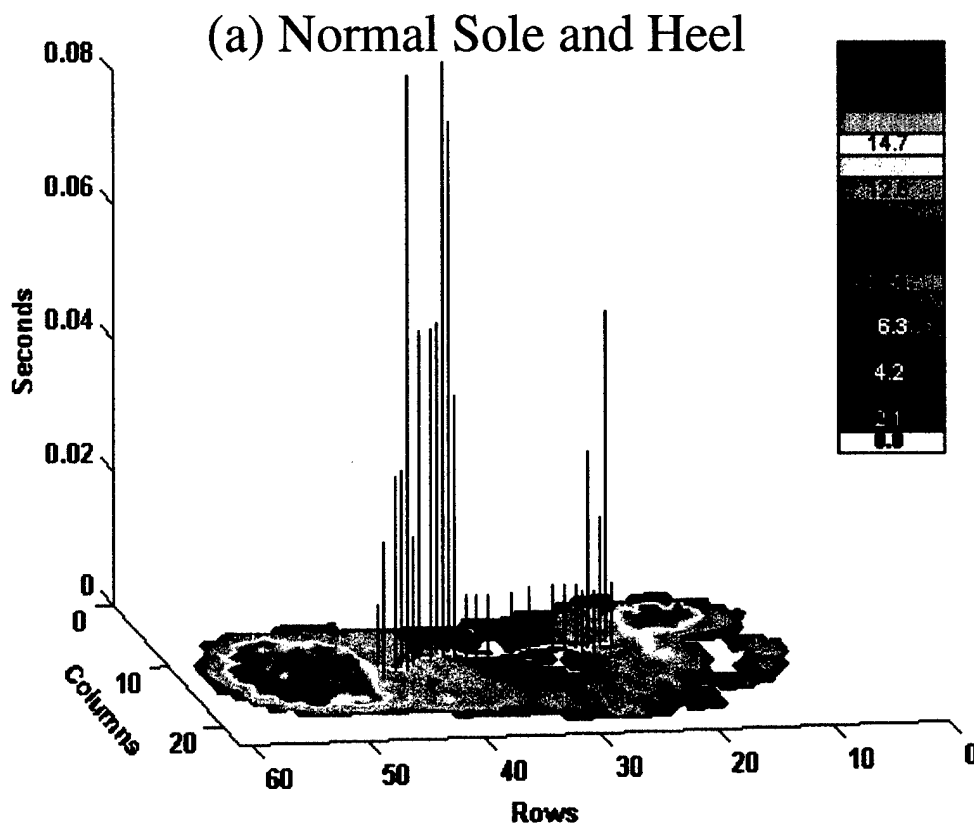
Figure 8. Peak plantar pressures over a gait cycle in the 10 m level walking trial of the neuromuscular test subject shown in Figure 7. Measurements were acquired using individual sensel calibrated, 960 element, FScan FVR insole transducers, sampled at 100 Hz. Pressures are shown color encoded by magnitude. Center of pressure (COP) trajectories are shown as a white line in the (x,y)–plane, with corresponding segmental temporal loading durations plotted along the z–axis. **(a)** In the shoes with standard width outer soles and heels, the subject is seen to initiate floor contact flatfooted, maintaining much of his body weight back on his heel throughout the weight transfer and midstance phases of gait. The subject's COP is seen to wander erratically, reflecting difficulty in neuromuscular control, and decreased stability. **(b)** With the extended width sole and heel shoes, loading is seen to be distributed more evenly over the subject's foot; he has more clearly demarcated heel contact and heel rise–to–toe off gait phases; and his COP trajectory is much smoother, indicating a stabler gait.

(a) Standard Shoes
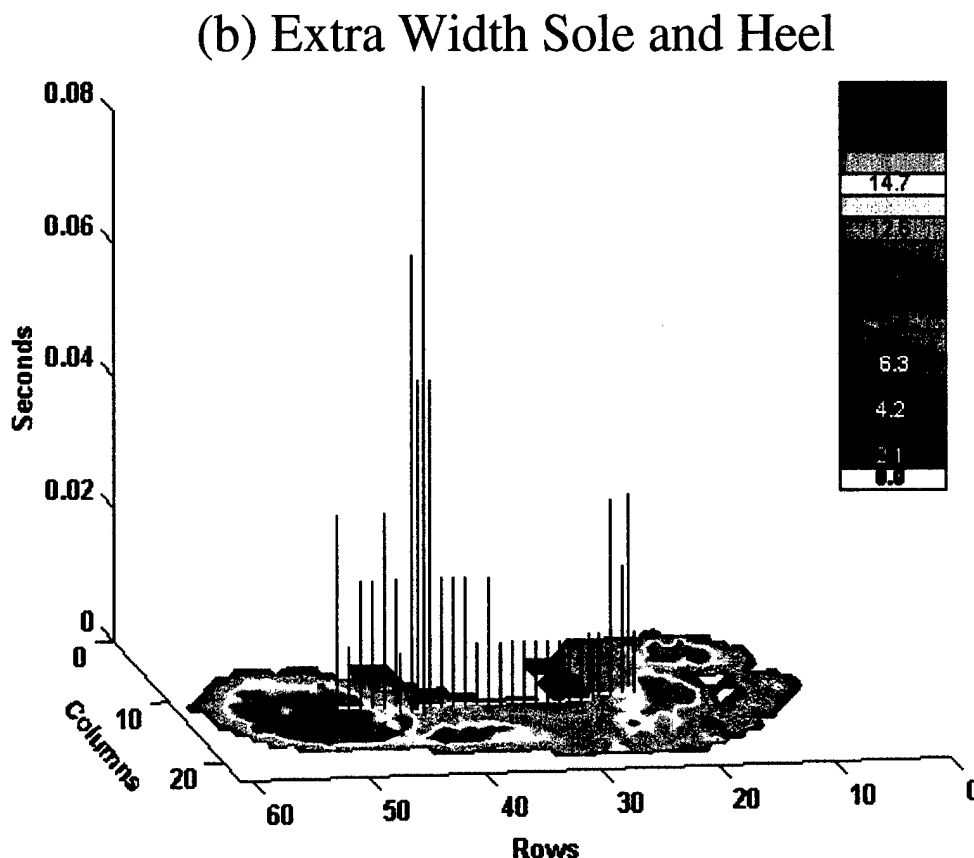
PARAMETER	tot/Left	Right
Leg Length(cm)	89.	89.
Step Time(sec)	.992	.972
Step Length(cm)	28.444	31.469
Step Extremity(ratio)	.32	.35
Cycle Time(sec)	1.963	1.982
Stride Length(cm)	59.94	61.359
HH Base Support(cm)	15.073	15.139
Swing Time(sec)	.565	.492
Stance Time(sec)	1.398	1.49
Single Supp. Time(sec)	.492	.565
Double Supp. Time(sec)	.912	.898
Swing % of Cycle	28.8	24.8
Stance % of Cycle	71.2	75.2
Single Supp % Cycle	25.1	28.5
Double Supp % Cycle	46.5	45.3
Toe In / Out	18.1	21.3

PARAMETER	
Step Count	24.
Distance	718.95
Ambulation Time	23.56
Velocity	30.5
Normalized Velocity	61.1
Cadence	.34
Step Time Differential	.02
Step Length Differential	3.025
Cycle Time Differential	.019
Functional Amb. Profile	55.

(b) Wide Soles

PARAMETER	tot/Left	Right
Leg Length(cm)	89.	89.
Step Time(sec)	.978	1.09
Step Length(cm)	29.106	32.063
Step Extremity(ratio)	.33	.36
Cycle Time(sec)	2.082	2.078
Stride Length(cm)	62.3	61.063
HH Base Support(cm)	10.536	10.332
Swing Time(sec)	.554	.58
Stance Time(sec)	1.528	1.498
Single Supp. Time(sec)	.58	.554
Double Supp. Time(sec)	.948	.945
Swing % of Cycle	26.6	27.9
Stance % of Cycle	73.4	72.1
Single Supp % Cycle	27.9	26.7
Double Supp % Cycle	45.5	45.5
Toe In / Out	16.8	24.1

PARAMETER	
Step Count	23.
Distance	701.97
Ambulation Time	23.74
Velocity	29.6
Normalized Velocity	58.1
Cadence	.33
Step Time Differential	.112
Step Length Differential	2.957
Cycle Time Differential	.004
Functional Amb. Profile	56.

Figure 9. GaitRite Electronic Walkway measurements over the 10 m level walking trial at user selected speed for the neuromuscular test subject in Figures 7 and 8: (a) in standard width sole and heel shoes, and (b) in extended width sole and heel shoes. In the extended width sole and heel shoes the subject's stride length is slightly increased; his mediolateral gait base decreased, and his COM mediolateral accelerations decreased — all indicative of an improved, more stable gait.
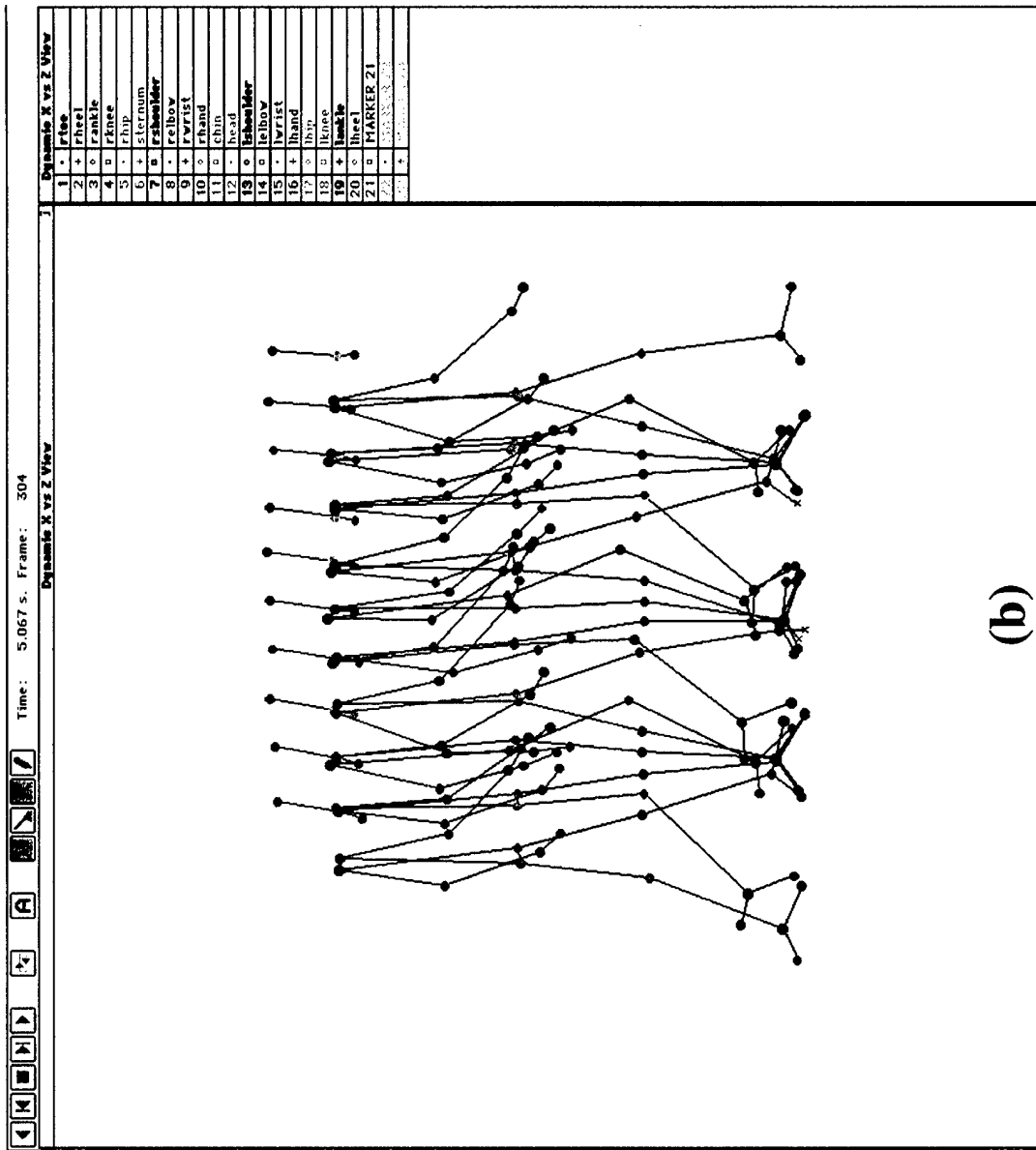
Figure 10. Biomechanical locomotion studies measuring pedal/footwear interface stresses, ground reaction forces, and body segment kinematics. (**a**) Coronal and sagittal views showing a pedorthic test subject in a 10 m level walking trial with rocker soled shoes, instrumented with 24 photoreflective markers at prescribed cranial, torso, and extremity locations for measurement of body segment spatiotemporal positions with the Qualisys 3-D Motion Analysis System. The subject is also instrumented with FScan plantar stress transducers, and is walking on the GaitRite Electronic Walkway and Kistler force plate which are simultaneously and synchronously recording ground reaction forces and spatiotemporal foot positions, velocities, and accelerations. (**b**) Sagittal view showing the stick figures characterizing the subject's spatiotemporal body segment kinematics generated by connecting the Qualisys System measurements of the photoreflective markers during the walking trial, and which are use to calculate the subject's respective body segment spatiotemporal positions, velocities, and accelerations over the trial.
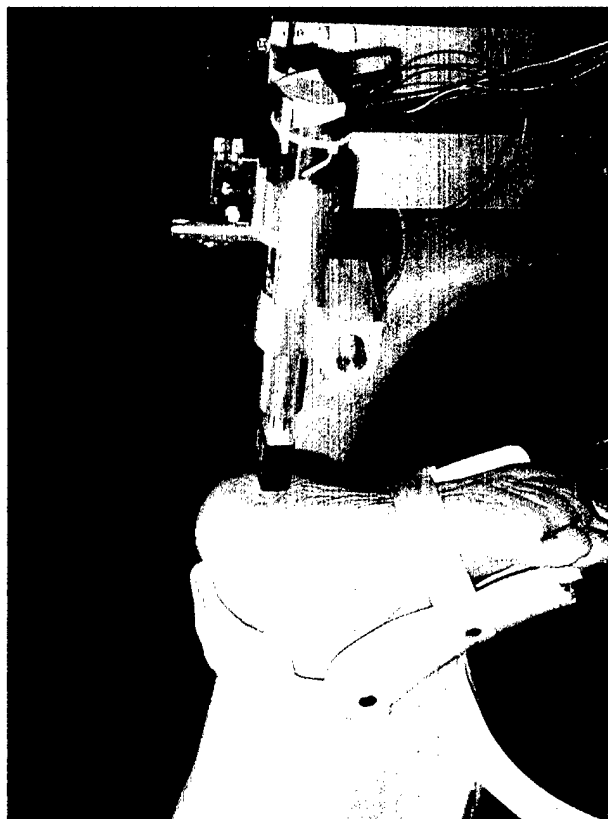
Pedorthic Patient Plantar Fat Pad Creep Response To Sequential, Calcaneal Step Loads

(b)

(a)

Steady State Creep Response at Plantar Fat Pad
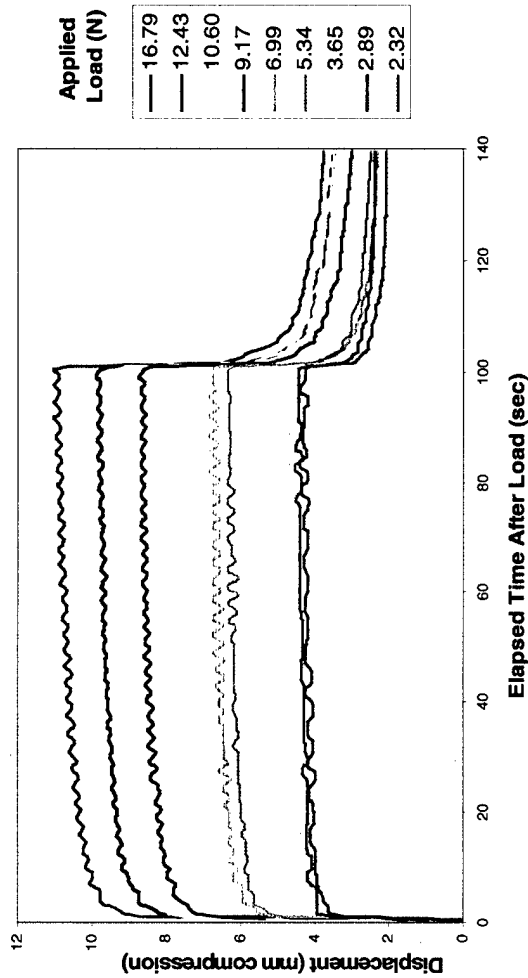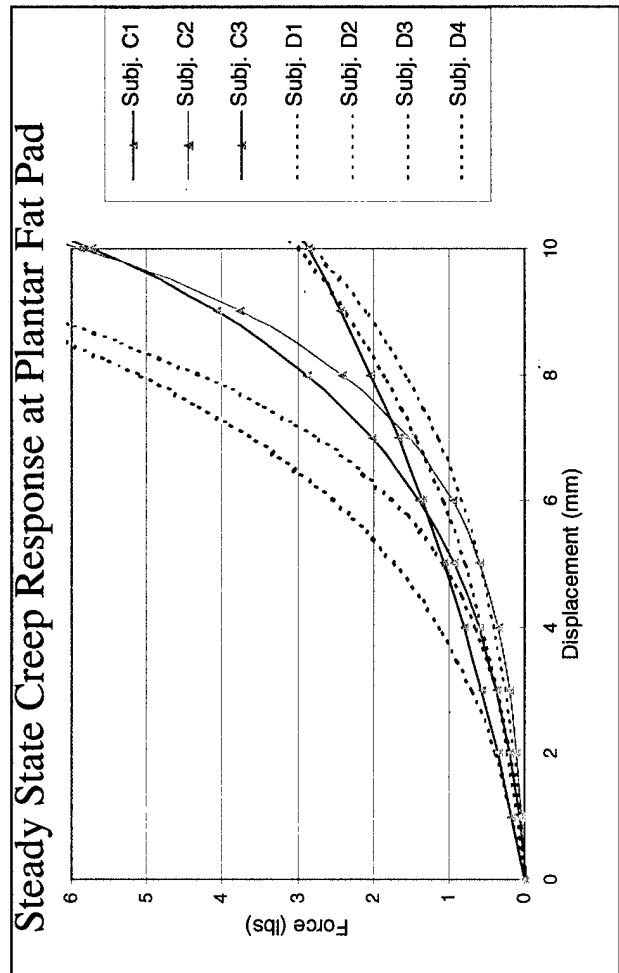
(c)

Figure 11. (A) Measurement of the mechanical properties of a pedorthic patients' pedal fat pad with the VA NYHHCS servo controlled, optoelectromechanical tissue indentor. As shown, subjects are mechanically "locked" in place relative to the indentor frame to mitigate "movement noise". (b) Tissue creep responses at nine step force loads of increasing magnitude, sequentially applied to the plantar fat pad. (c) Resulting Force-Displacement plots of the steady state creep response of the pedal plantar fat pads for 3 normal subjects, and 4 neuropathic diabetic subjects.
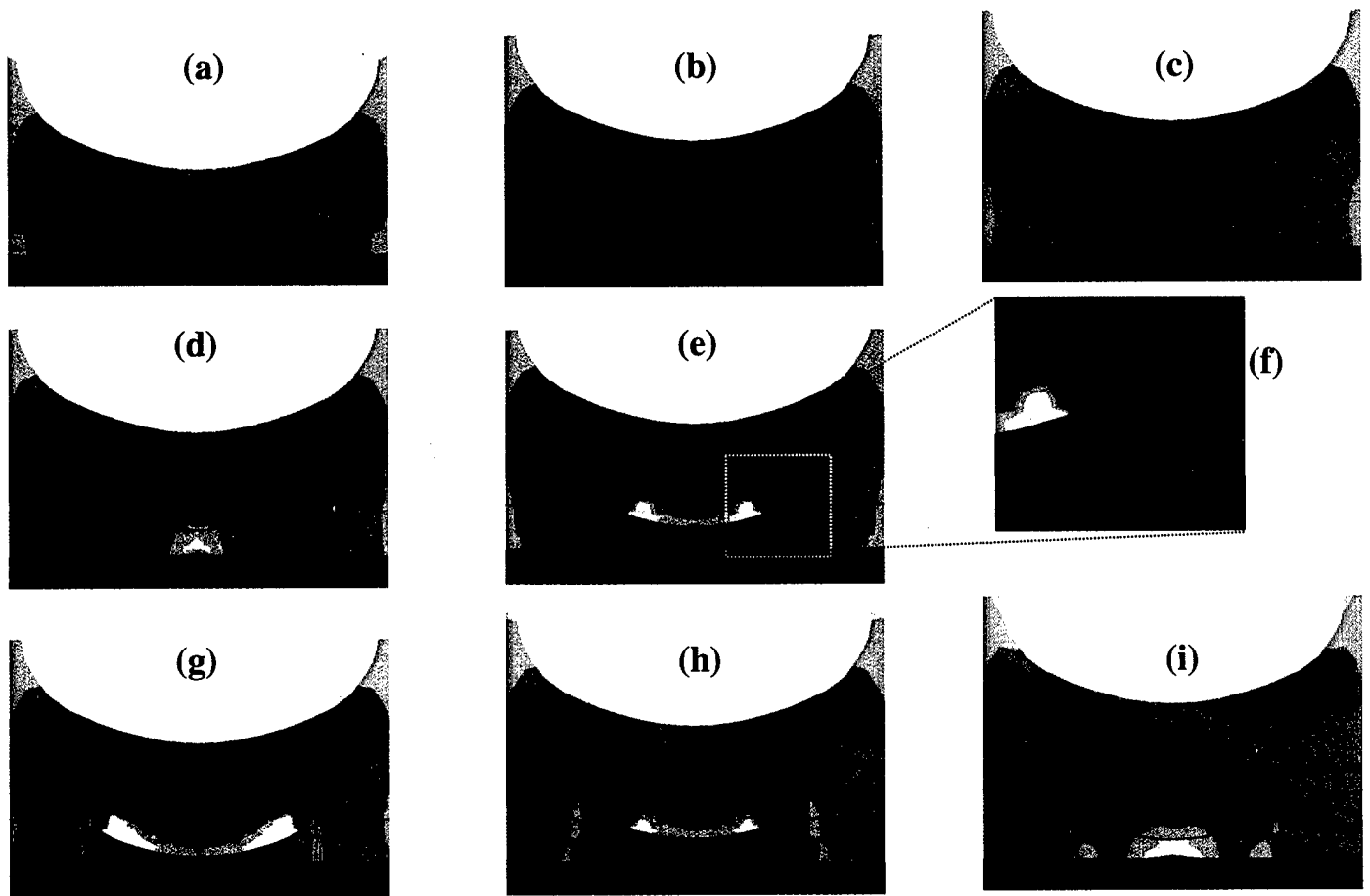
Figure 12. Optimization of pedorthic treatment for podalgia/plantar fasciitis — pedal plantar tissue stress. Mid-calcaneal, frontal cross sections of the foot of a test subject showing FEA predicted vertical stress incurred, as a function of pedorthic insole material stiffness and design geometry, when the subject stands on a flat, rigid surface, applying a vertical load of 200 Newtons (approximately ¼ body weight) through his talus and calcaneous. All insoles in their unloaded state are 5 mm thick at center. (a) Tissue stress distribution incurred with the subject standing barefoot without a pedorthosis. (b) Tissue stress distribution incurred with the subject standing on a non-contoured, generic insole, with material stiffness equivalent to that of his pedal tissues. (c) Stress distribution incurred when standing on a non-contoured insole with material stiffness six times that of his pedal tissue. (d) Stress distribution produced by standing on a non-contoured, generic insole, six times pedal tissue stiffness, with a conical relief 25 mm in base diameter and 2.5 mm deep cut out of the bottom of the insole under the heel. (e) Stress distribution produced by standing on a non-contoured insole, six times pedal tissue stiffness, with a 14 mm diameter cylindrical relief cut out of the insole under the heel. (f) Enlarged inset of case (e) showing the increase in stress magnitudes due to the Dunnel effect from large gradients in stiffness of adjoining materials at the tissue–insole–relief junction. (g) Stress distribution produced with a non-contoured insole, six times pedal tissue stiffness, with a 20 mm diameter cylindrical relief cut out under the heel. (h) Stress distribution produced with an insole six times pedal tissue stiffness, and custom made to match the subject's pedal contours, with a 14 mm diameter cylindrical relief cut out under the heel. (i) Stress distribution produced with a custom contoured insole, six times the pedal tissue stiffness, with a conical relief 25 mm in base diameter and 2.5 mm deep cut out under the heel, and with the additional condition that rheological displacement of pedal soft plantar tissues relative to the calcaneous is constrained (as achieved by extending the borders of the insole proximally around the fat pad to hold it in place). As clearly evident, only in this latter case are tissue stresses and stress gradients reduced appreciably. *(See Table 3 for a quantitative tabulation of results.)*

Stress (MPa)

1.000e-001
5.000e-002
0.000e+000
-5.000e-002
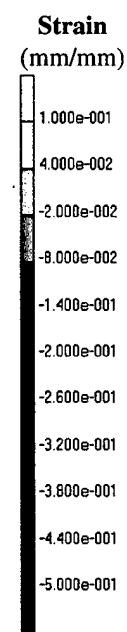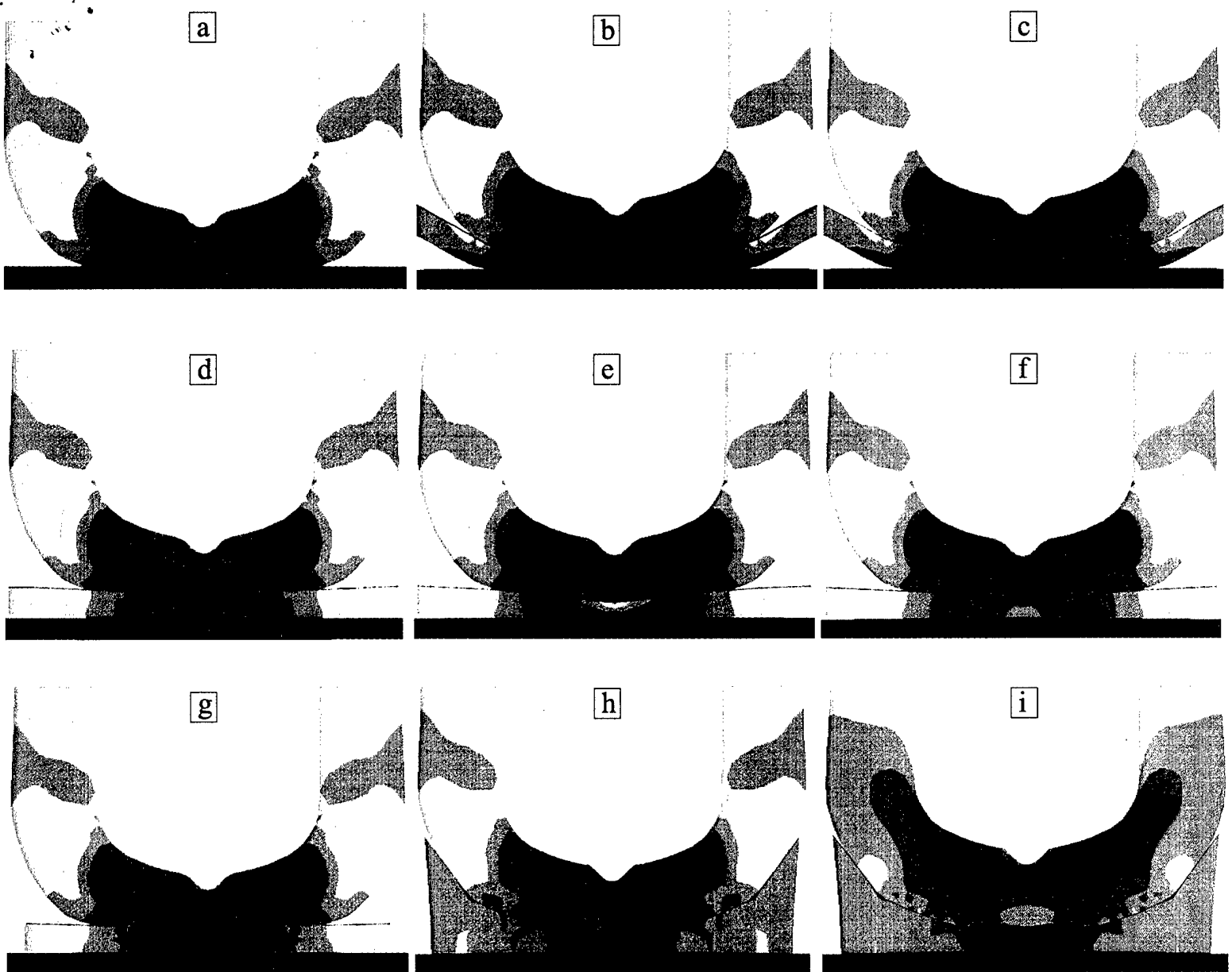-1.000e-001
-1.500e-001
-2.000e-001
-2.500e-001
-3.000e-001
-3.500e-001
-4.000e-001
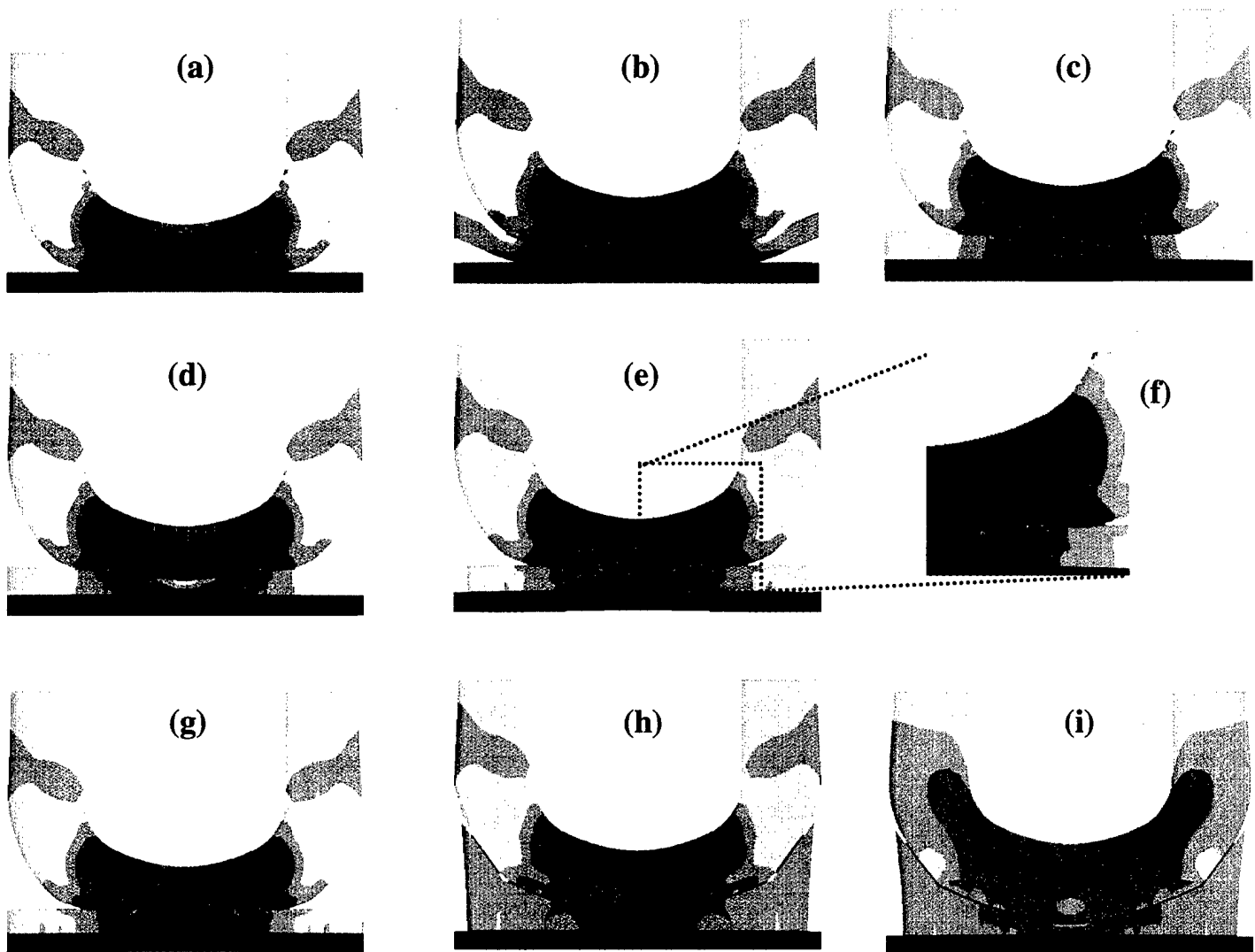
Figure 13. Optimization of pedorthic treatment for podalgia/plantar fasciitis — pedal plantar tissue strain. FEA predicted tissue total vertical strains at the mid-calcaneal, frontal cross section of the test subject's foot in Figure 12, standing on a flat, rigid surface supporting a 200 Newton vertical load through his calcaneous and talus. (a) Tissue strains incurred standing barefoot without a pedorthosis. (b) Tissue strains incurred when standing on a non-contoured, generic insole with material stiffness equivalent to that of the subject's pedal tissues. (c) Strains incurred when standing on a non-contoured insole with material stiffness six times that of pedal tissue. (d) Tissue strains produced by standing on a non-contoured insole, six times pedal tissue stiffness, with a conical relief 25 mm in base diameter and 2.5 mm deep cut out of the bottom of the insole under the heel. (e) Strains produced by standing on a non-contoured insole, six times pedal tissue stiffness, with a 14 mm diameter cylindrical relief cut out of the insole under the heel. (f) Enlarged inset of case (e) showing the strains and strain gradients produced adjacent to the insole relief border. (g) Strains produced with a non-contoured insole, six times pedal tissue stiffness, with a 20 mm diameter cylindrical relief cut out under the heel. (h) Strains produced with an insole six times pedal tissue stiffness, and custom fabricated to match the subject's pedal contours, with a 14 mm diameter cylindrical relief cut out under the heel. (i) Strains produced with a custom contoured insole, six times pedal tissue stiffness, with a conical relief 25 mm in base diameter and 2.5 mm deep cut out under the heel, and with the additional condition that rheological displacement of pedal soft plantar tissues relative to the calcaneous is constrained (as achieved by extending the borders of the insole proximally around the fat pad to hold it in place). As evident, only in this latter case are tissue strains reduced appreciably.

Strain
(mm/mm)

1.000e-001
4.000e-002
-2.000e-002
-8.000e-002
-1.400e-001
-2.000e-001
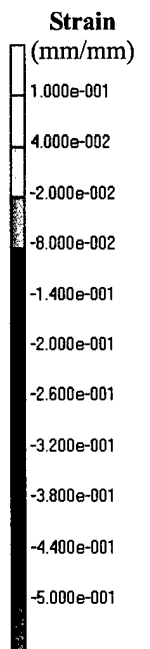-2.600e-001
-3.200e-001
-3.600e-001
-4.400e-001
-5.000e-001

Figure 14. Optimization of pedorthic treatment for calcaneal osteophytes pedal plantar tissue strain. FEA predicted tissue total vertical strains at the mid-calcaneal, frontal cross section of the foot of a test subject with a vertical heel spur, standing on a flat, rigid surface, applying a 200 Newton vertical load through his talus and calcaneous. Tissue strains are shown as a function of pedorthic insole material stiffness and design geometry. All insoles are 5 mm thick at center in their unloaded state. **(a)** Tissue strains incurred with the subject standing barefoot without a pedorthosis. **(b)** Tissue strains incurred when standing on a non-contoured, generic insole with material stiffness equivalent to that of the subject's pedal tissues. **(c)** Strains incurred when standing on a non-contoured insole with material stiffness 2.5 times that of pedal tissue. **(d)** Tissue strains produced by standing on a non-contoured insole, six times pedal tissue stiffness. **(e)** Tissue strains produced by standing on a non-contoured insole, six times pedal tissue stiffness, with a conical relief 25 mm in base diameter and 2.5 mm deep cut out of the top of the insole under the heel. **(f)** Tissue strains produced by standing on a non-contoured insole, six times pedal tissue stiffness, with a conical relief 25 mm in base diameter and 2.5 mm deep cut out of the bottom of the insole under the heel. **(g)** Strains produced by standing on a non-contoured insole, six times pedal tissue stiffness, with a 14 mm diameter cylindrical relief cut out of the insole under the heel. **(h)** Strains produced with an insole six times pedal tissue stiffness, and custom fabricated to match the subject's pedal contours, with a 14 mm diameter cylindrical relief cut out under the heel. **(i)** Strains produced with a custom contoured insole, six times pedal tissue stiffness, with a 14 mm diameter cylindrical relief cut out under the heel, and with the additional condition that rheological displacement of pedal soft plantar tissues relative to the calcaneous is constrained (as achieved by extending the borders of the insole proximally around the fat pad to hold it in place). Only in the latter case are pedal tissue strains reduced appreciably. *(See Table 4 for a quantitative tabulation of results.)*

Strain
(mm/mm)

1.000e-001

4.000e-002

-2.000e-002

-8.000e-002

-1.400e-001

-2.000e-001

-2.600e-001

-3.200e-001

-3.800e-001

-4.400e-001

-5.000e-001

Plastic Insole Material Stress-Strain Characteristics
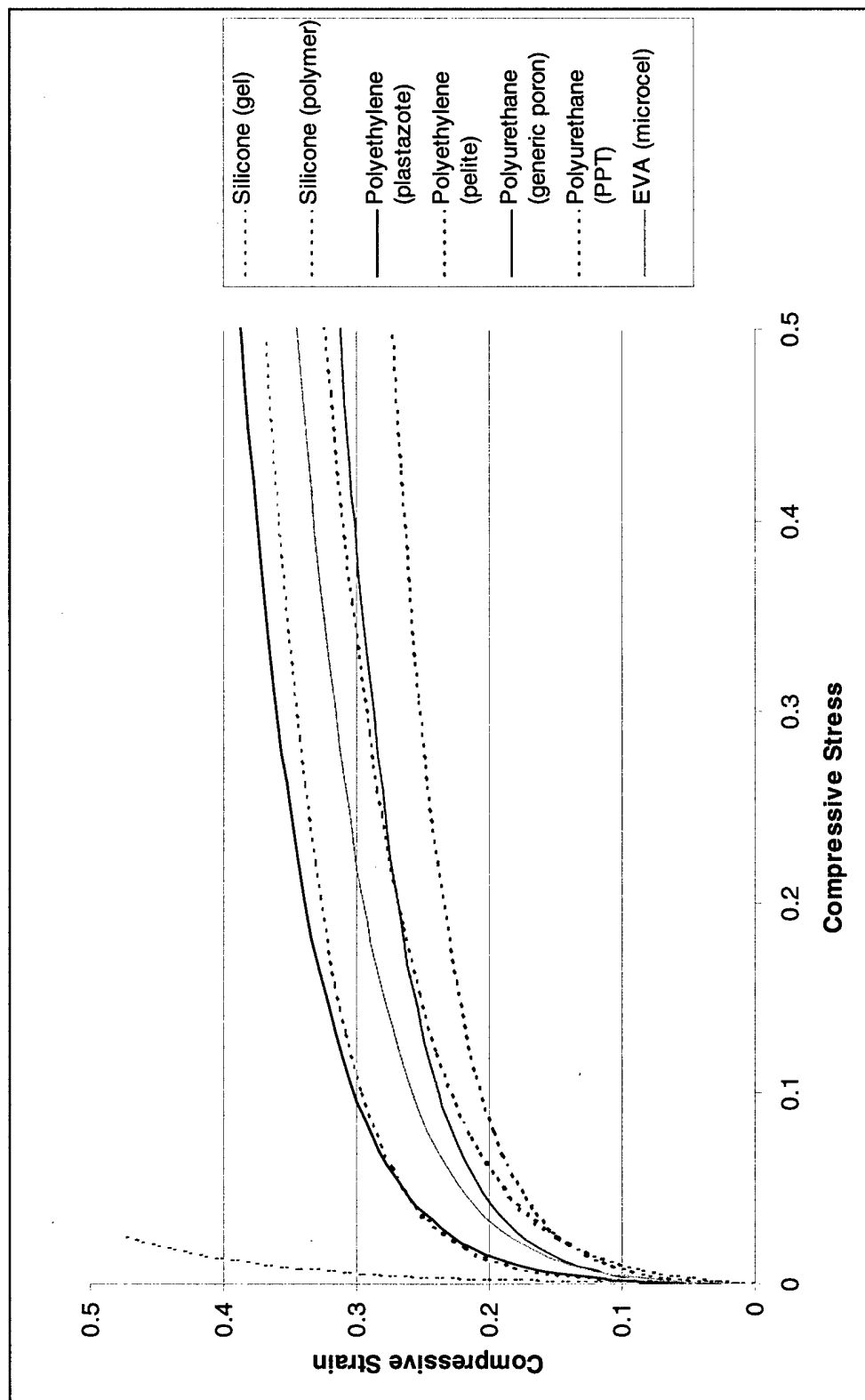
Figure 15. Nonlinear stress-strain characteristics of seven plastic materials commonly used in fabrication of orthopedic insoles.
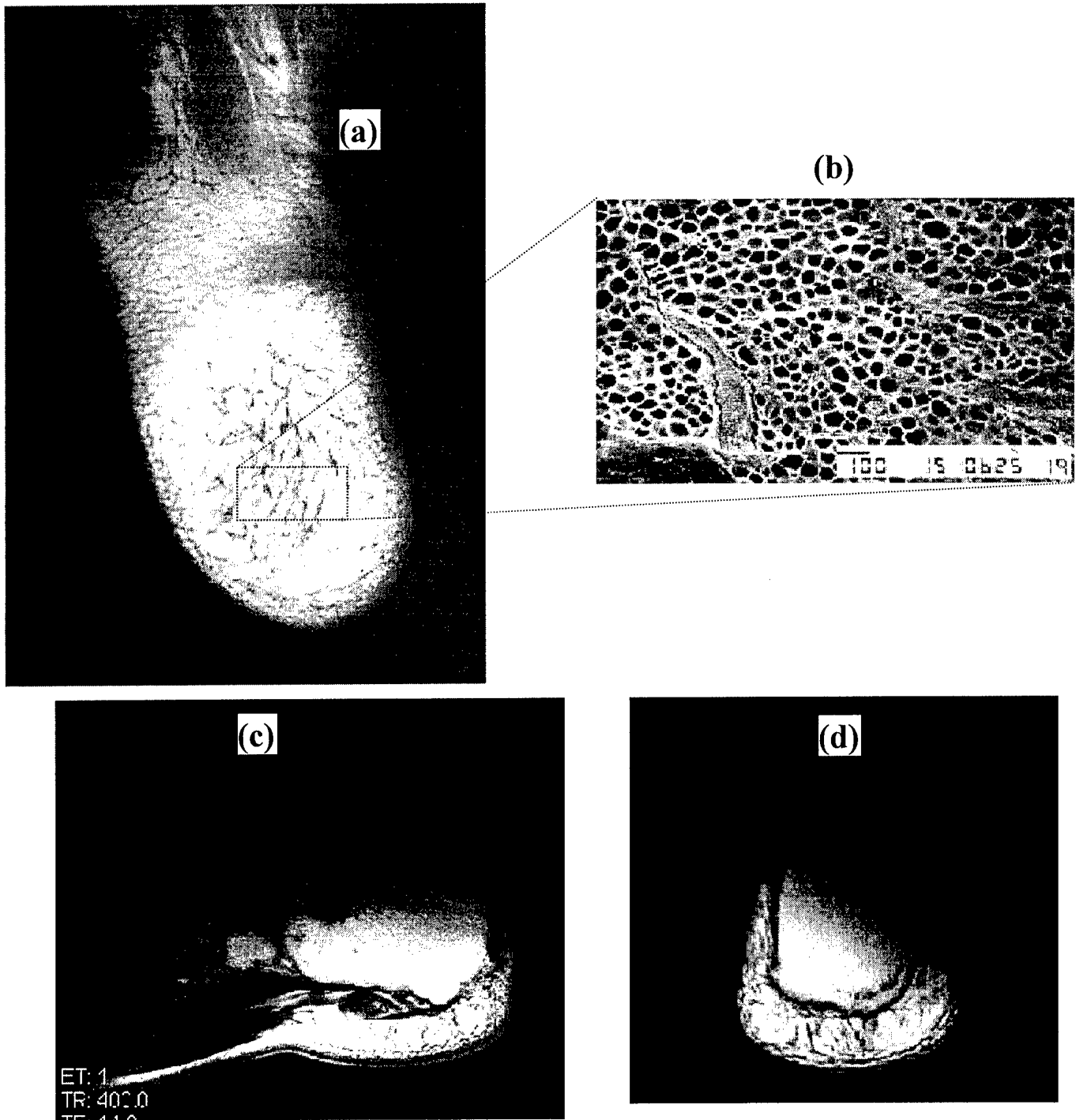
Figure 16. Magnetic resonance images of a test subject's foot in an unloaded state, showing: **(a)** a longitudinal cross section distal to the calcaneous **(b)** a magnified histological section of the plantar fat pad under the calcaneous, showing the individual, "honey comb" like septae that dampen and disperse pedal loads; **(c)** a sagittal cross section through the mid-foot showing the morphology of the fat pad, plantaraponeurosis, calcaneous, and talus; and **(d)** a frontal cross section through the mid-calcaneous showing the relative structure of the fat pad, with axial alignment of the septae directly under the calcaneousfor damping of impact loads, and gradual transition of the septal alignment to a convoluted pattern near the calcaneal borders serving to disperse plantar loading.
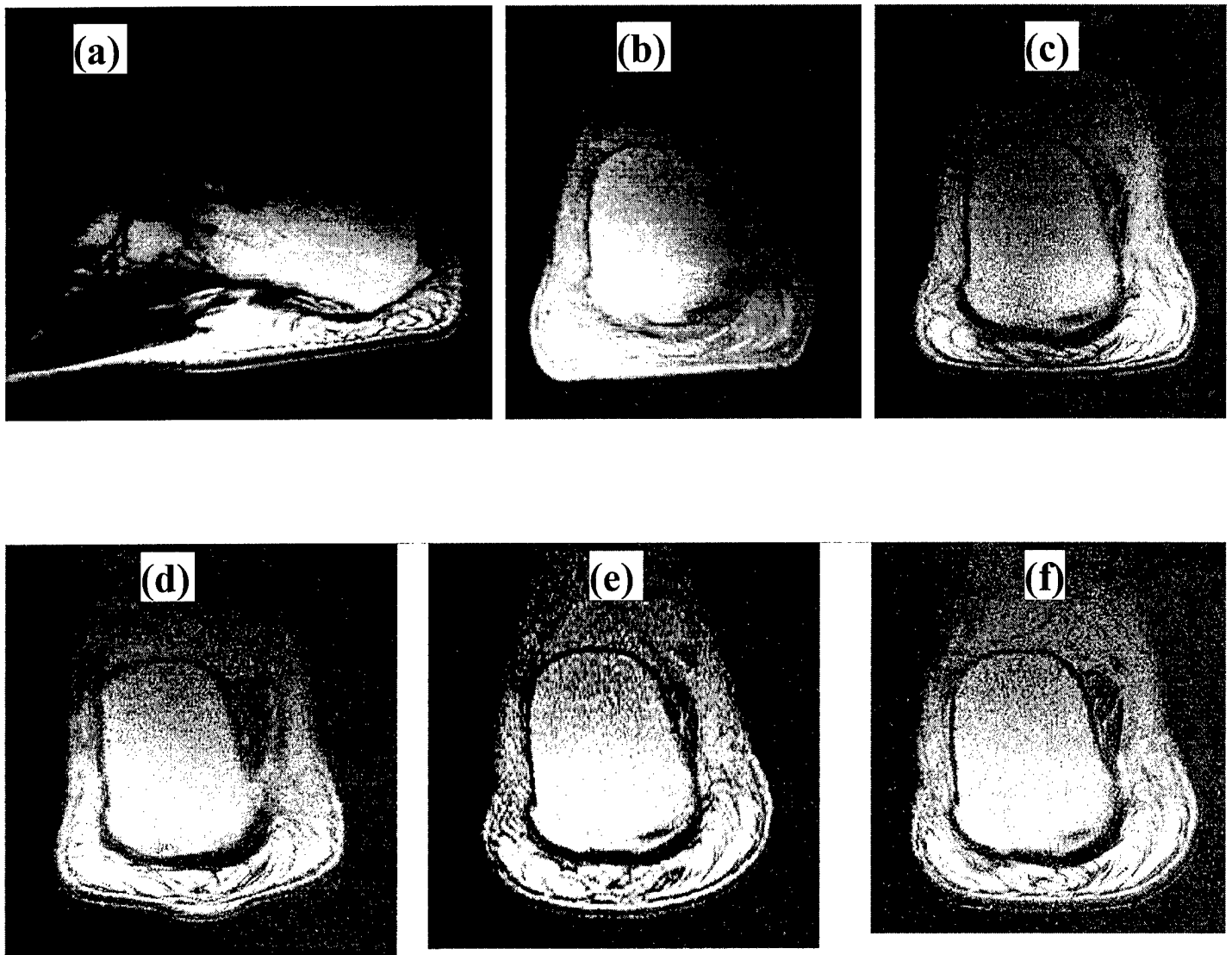
Figure 17. Magnetic resonance images of the test subject's foot in Figure 16 with a 200 Newton load applied axially through the tibia, talus, and calcaneous **(a)** Sagittal cross section of the subject's foot axially loaded without a pedorthosis.**(b)** Frontal cross section through the mid-calcaneous of the subject's bare foot under axial load.**(c)** Frontal cross section of the subject's foot under axial load while supported on a generic, non-contoured insole, approximately six times his pedal tissue stiffness.**(d)** Frontal cross section of the subject's foot under axial load while supported on a generic, non-contoured insole, approximately six times his pedal tissue stiffness, with a 14 mm diameter cylindrical relief cut out under the heel. **(e)** Frontal cross section of the subject's foot under axial load while supported on a custom contoured insole designed to match his unloaded pedal tissue shape, approximately six times his pedal tissue stiffness. **(f)** Frontal cross section of the subject's foot under axial load while supported on an insole approximately six times his pedal tissue stiffness, custom contoured to match his unloaded pedal shape, with borders extending proximally, constraining displacement of his pedal plantar fat pad. The tissue strains incurred with the custom contoured insoles are seen to be measurably less than with the non-contoured, generic insoles.

Table 1. VA OSS ORTHOPEDIC SHOE LAST SURVEY MODIFICATION CODE LOG

LAST REGION	MOD CODE	MAGNITUDE AND/OR DIRECTION OF MODIFICATION	LAST REGION	MOD CODE	MAGNITUDE AND/OR DIRECTION OF MODIFICATION
1 TOE BOX AREA	A	RAISED 0 TO 1/4" DORSAL	6 FOREFOOT POSITION	A	ADDUCTED
	B	RAISED 1/4 TO 1/2 "		B	ABDUCTED
	C	RAISED 1/2 TO 1 "		C	BUNION SHAPE
	D	WIDER WIDTH 0 TO 1/4 "		D	STRAIGHT
	E	WIDER WIDTH 1/4 TO 1/2 "			
	F	WIDER WIDTH 1/2 TO 1 "	7 TONGUE/VAMP	A	BUILDUP 0 TO 1/4 "
	G	ADDITION TO PLANTAR AREA 0 TO 1/4 "		B	BUILDUP 1/4 TO 1/2 "
	H	ADDITION TO PLANTAR AREA 1/4 TO 1/2 "		C	BUILDUP 1/2 TO 1 "
	I	ADDITION TO PLANTAR AREA 1/2 TO 1 "			
2 HALLUX AREA	A	RAISED DORSAL 0 TO 1/4 "	8 HEEL AREA	A	PLANTAR AREA DEPRESSION 0 TO 1/4 "
	B	RAISED DORSAL 1/4 TO 1/2 "		B	PLANTAR AREA DEPRESSION 1/4 TO1/2 "
	C	RAISED DORSAL 1/2 TO1 "		C	PLANTAR AREA DEPRESSION 1/4 TO 1 "
	D	WIDEN AREA 0 TO 1/4 " MED SIDE		D	PLANTAR AREA RAISED 0 TO 1/4 "
	E	WIDEN AREA 1/4 TO 1/2 " MED SIDE		E	PLANTAR AREA RAISED 1/4 TO1/2 "
	F	WIDEN AREA 1/2 TO 1 " MED SIDE		F	PLANTAR AREA RAISED 1/2 TO 1 "
	G	PLANTAR AREA RAISED 0 TO 1/4 "		G	LATERAL WEDGE 0 TO 1/4 "
	H	PLANTAR AREA RAISED 1/4 TO1/2 "		H	BUILDUP AROUND HEEL M/L 1/4 "
	I	PLANTAR AREA RAISED 1/2 TO 1 "			
3 5TH TOE AREA	A	RAISED DORSAL 0 TO 1/4 "	9 HEEL POSITION	A	STRAIGHT
	B	RAISED DORSAL 1/4 TO 1/2 "		B	INVERSION
	C	RAISED DORSAL 1/2 TO1 "		C	EVERSION
	D	WIDEN AREA 0 TO 1/4 " LAT SIDE			
	E	WIDEN AREA 1/4 TO 1/2 " LAT SIDE	10 PLANTAR SURFACE	A	RAISE UNDER TOES (S,M,L)
	F	WIDEN AREA 1/2 TO 1 " LAT SIDE		B	RAISE UNDER METHEADS (S,M,L)
	G	PLANTAR AREA RAISED 0 TO 1/4 "		C	DEPRESSION UNDER TOES (S,M,L)
	H	PLANTAR AREA RAISED 1/4 TO1/2 "		D	DEPRESSION UNDER METHEADS (S,M,L)
	I	PLANTAR AREA RAISED 1/2 TO 1 "		E	WEDGE LATERAL SIDE OF FOOT (S,M,L)
4 METATARSAL AREA	A	PLANTAR AREA DEPRESSION 0 TO 1/4 "		F	WEDGE MEDIAL SIDE (S, M, L)
	B	PLANTAR AREA DEPRESSION 1/4 TO1/2 "		G	(S) 1/4SMALL , (M) 1/2MED (L) 3/4 LARGE
	C	PLANTAR AREA RAISED 0 TO 1/4 "		H	OTHER THAN ABOVE
	D	PLANTAR AREA RAISED 1/4 TO1/2 "			
5 ARCH AREA	A	PLANTAR AREA DEPRESSION 0 TO 1/4 "	11 ANKLE	A	BUILDUP MED 0 TO 1/2"
	B	PLANTAR AREA DEPRESSION 1/4 TO1/2 "		B	BUILDUP LAT 0 TO 1/2"
	C	PLANTAR AREA DEPRESSION 1/4 TO 1 "		C	BUILDUP BILATERALLY 0 TO 1/2"
	D	PLANTAR AREA RAISED 0 TO 1/4 "		D	BUILDUP > 1/2" M(MED, L(LAT) B(BOTH)
	E	PLANTAR AREA RAISED 1/4 TO1/2 "			
	F	PLANTAR AREA RAISED 1/2 TO 1 "			

Table 2. Female Test Subject — Foot/Ankle Manual Measurements

Sub No	Body H	Calf C	Heel Toe L	Heel Ball L	Heel Ant. Ankle L	Heel Lever	Toe Lever	Ball W Horiz	Ball W Dia	Heel to 5MTH	Heel W	Ball C	Waist C	Heel to Instep L	Instep C	Span C	Heel Toe Semi C	Max Toe H	Ankle H	Ankle AP W	Ankle ML W	Ankle C	Malleolus L-R	M Malleolus H	L Malleolus H	Dorsal Foot H/H	M Plan Arch H
1	168	37	24.5	17	10.5	6.2	17.3	9.5	10.5	16.2	7.37	26.9	26.5	10.5	29	34.5	27	3	10	9.37	6.8	27	6.9	8.5	7	7.8	1.9
2	178	30	25.8	18.3	9.3	6	20	9.6	10.1	17.5	6.3	24.4	24	11	24.1	34	28	2.6	11	8.9	7	24	6.8	9	7.8	7.6	4
3	160	27	24	17.5	8	4.6	18.5	8.9	9	16.1	6.2	20.6	21.5	9.5	21.8	30.8	25.7	2.5	9.3	7.1	6.2	19	6.6	7.83	6.13	6.6	2.3
4	164	28	22.6	17.1	8	5.7	16.9	8.1	8.2	14.36	5.9	21	19.7	11	20.4	29	25	2.2	9.1	7.3	5.3	20		7.28	5.58	5.9	2.9
5	161	32	24.2	17.4	8.6	4.5	19.7	9.2	9.53	14.14	6.1	24.5	22.8	10.1	24	31.3	25.3	2.3	10	8.2	5.4	22	6.7	7.7	6.68	6.5	2.7
6	159	32	23	16.5	10	5.1	13	9.1	9.5	14	6.4	23	23.1	10.6	24.2	31.1	26	2.7	10	7.6	6.1	21	6.2	7.4	7.4	7.3	2.6
7	155	38	23.2	17.3	10.5	6.5	16.7	9.6	10	14.5	5.8	23.6	23.8	12	24.1	31.9	25.6	2.8	9.7	8.1	7	23	6.7	8.25	6.84	7.2	4
8	157	31	22.9	16.7	9	4.5	18.4	8.2	8.9	14.5	5.9	21.1	20.7	11	21.8	30.3	26.2	2.8	8.5	7	5.6	21	6	8.38	6.4	6.5	2.9
9	157	34	23.6	16.9	8.5	4.7	18.6	8.9	9.1	14.7	5.7	21.2	21.1	11.4	22	31.2	25.6	2.8	10	6.7	5.2	20	5.8	8.77	6.55	7.2	3.4
10	171	30	23.4	17.1	7.7	5.7	17.7	8.5	8.6	15.6	5.2	21.3	20.7	9.3	21.9	31.5	26.5	2.4	11	6.5	4.9	20	6.4	8.63	6.8	7	3.7
11	165	32	25	18.4	8.8	5.4	19.6	9	9.1	16.6	5.9	22.1	21.9	10	22.9	31.4	31.4	2.4	10	6.6	5.5	20	6.8	8.24	6.98	6.5	3.1
12	154	32	22.8	17.1	9	5.5	17.3	8	8.2	14.9	5.5	20	19.8	9.9	21.9	28.4	25.5	2.2	9.4	6.8	5.2	20	6	7.38	6.61	6.2	3.1
13	163	33	24.1	17.4	9	5	15	8.8	8.9	15.5	6.1	22.1	22.5	11	23.4	32.4	27.1	2.7	10	6.8	6	21	6.1	8.08	7.1	7	3.4
14	165	30	22.6	17	8.5	5.5	17.1	8	8.1	14.3	5.1	20	20.4	10.4	20.5	31.1	25.6	2.5	10	6.6	5	19	5.8	7.86	6.2	6.1	2.7
15	160	33	22.6	16.9	7.8	6.3	16.3	8.3	8.6	14.4	5.5	21.6	21.4	9.9	22.8	30.3	25.7	2.1	9.7	6.5	5.5	20	6.4	7.42	6.53	6.5	2.8
16	173	38	25.9	19.4	10	6.4	19.5	9.6	9.8	17.1	6.5	24.5	25	11.6	25.1	36.8	29.1	3.7	12	7.9	6.1	24	7	9.67	7.62	7	3.4
17	165	29	24.7	18.1	10	6.3	18.4	9	9.1	16.4	6.8	22.9	22.7	12.3	23	33.9	29.2	3.1	10	7.6	5.6	21	6.3	8.43	6.87	6.8	3.1
18	160	31	22.6	16.4	8.5	5.5	17.1	9.3	9.4	14.5	5.5	22.1	21.1	10.6	21.8	30.9	25.1	2	9.3	6.4	5.1	19	6	7.3	6.53	6	2.1
19	165	32	24.9	17.8	9	5.5	19.4	9.6	9.3	15.5	6.2	23	23	11	23.6	31.6	27.1	2.6	9.9	7.5	5.8	22	6.3	8.17	6.92	6.7	2.4
20	173	32	24.5	18.2	9.7	6	18.5	8.9	9.2	15.4	6.5	23.4	22.3	11.6	24	34.3	26.6	3.2	11	7.8	6.2	23	6.3	8.58	7	7.5	3.9
21	152	35	22.5	16.2	8.7	5.2	17.3	8.9	9	13.8	5.7	23.4	22.8	9.6	23.9	31.3	24.5	2.9	10	7.5	5.9	22	6.8	8.32	6.61	7	3.1
22	163	37	23.7	17.6	8.8	6	17.7	8.7	8.8	14.9	6	22.7	22.4	11.5	23.4	33.2	27	2.5	11	8.5	6.6	25	6.5	8.97	6.76	7.2	3
23	160	32	24	17.9	8.9	6.4	17.6	8.6	8.9	15.2	5.8	22	21.6	10.9	23	32.7	26.9	2.9	10	7.1	5.4	21	6.3	7.67	7.23	7.3	2.3
24	175	32	25.4	18.5	9.6	6.4	19	9.2	9.3	16.6	5.7	23.4	22.5	12.5	23.5	32.4	27.7	2.4	11	7.5	5.4	21	7.3	8.58	6.49	7.2	2.3
25	161	31	24.5	17.8	8.2	6	18.5	9.1	9.5	14.5	6.5	22.6	22.6	12	24.1	33.9	27.3	2.7	11	7.3	5.2	21	6	8.59	6.36	7.6	2.8
26	171	40	25.4	19.7	9.4	7.6	17.8	10.2	10.4	16.6	7.6	25.9	26.7	12.9	26.6	35.8	29.5	3.7	10	8.6	6.8	25	7.5	8.03	7.07	6.7	1.5
27	157	34	23.4	17.4	8.6	5.6	17.8	9.7	9.8	14.6	5.5	23.7	22.3	10.7	23.2	32.8	27	2.8	11	7.6	5.9	22	6.4	8.3	7.39	7.5	3.5
28	165	29	24.8	18.1	7.8	4.9	19.9	8.9	9	16.1	6.3	22	22.4	10.7	23.9	32.2	27.3	2.2	9.9	6.9	5.5	20	6.6	7.59	7.31	6.8	1.6
29	171	27	26.5	19.6	10.5	7.4	19.1	9.5	9.8	17.6	7.3	25	25	13.1	26.3	38.8	30.8	2.8	11	7.5	5.6	22	6.6	9.12	7.07	8.4	3.2
30	168	32	24.6	18	7.1	5.5	19.1	9.2	9.3	15.4	6.2	23.4	22.7	11.9	24.5	33.6	28.1	2.6	11	7.7	6.5	23	6.6	9.1	7.73	7.7	3
31	165	31	24.4	17.6	8.6	6.4	18	8.8	8.9	15.6	6	22.8	22.2	11.8	23	31.2	27.1	2.8	9.9	7.5	5.8	21	6.8	8.3	7.07	7.2	2.7
32	160	29	23.8	17.8	8.8	5.9	17.9	9.2	9.3	15	6.3	22.1	22	10.5	22.8	31.5	26	2.3	9.7	6.9	5.9	21	6.5	7.88	7.56	6.6	2.1
33	157	34	22.6	16.6	7.8	5.9	16.7	9.5	9.1	13.4	6.4	22.5	22.4	10.9	22.7	30.3	26.1	2.6	9.3	6.8	5.6	21	6.3	7.55	5.88	6.3	2.6
34	157	36	22.5	16	8.1	5.5	17	8.7	8.9	13.9	5.2	22.3	22	10.4	22	30.1	24.6	2.4	9.8	7.1	5.4	20	6.6	7.98	6.5	7	2.7
35	165	32	24.8	18.1	9.8	6.5	18.3	8.5	8.9	15	5.7	33.5	22	10.9	25	32.1	26	2.3	11	7.5	5.1	20	6.5	8.5	6.78	7.8	3

Table 3. Optimization of Pedorthic Treatment for Podalgia
Stresses–Strains in Heel Pad Soft Tissue vs Pedorthic Insole Stiffness & Geometry

Pedorthic Insole	Heel Pad Maximum Cauchy Stress (MPa)	Heel Pad Maximum Green Strain (mm/mm)	Heel Pad Maximum Strain Energy Density ($x10^{-3}$ Joule / mm^3)
(a) No Insole	−0.412	−0.459	53.06
(b) Standard flat insole with 1x stiffness of heel pad tissue	−0.354	−0.445	33.77
(c) Standard flat insole with 2.5 x stiffness of heel pad tissue	−0.378	−0.452	40.90
(d) Standard flat insole with 6 x stiffness of heel pad tissue	−0.394	−0.455	46.27
(e) Standard flat insole with 6 x tissue stiffness & 25mm base diameter 2.5mm deep conical relief on bottom surface	−0.342	−0.438	30.44
(f) Standard flat insole with 6 x tissue stiffness & 25mm base diameter 2.5mm deep conical relief on top surface	−0.341	−0.436	30.06
(g) Standard flat insole with 6 x tissue stiffness & 20mm diameter cylindrical relief	−0.277	−0.400	13.08
(h) Standard flat insole with 6 x tissue stiffness & 14mm diameter cylindrical relief	−0.344	−0.434	30.87
(i) Custom contoured insole with 6 x tissue stiffness & 14mm diameter cylindrical relief	−0.236	−0.384	8.91
(j) Custom contoured insole with 2.5 x tissue stiffness & 14mm diameter cylindrical relief	−0.234	−0.381	8.84
(k) Custom contoured insole with 6 x tissue stiffness, 20mm diameter cylindrical relief	−0.197	−0.344	5.76
(l) Custom contoured insole with 6 x tissue stiffness, 25mm base diameter 2.5mm deep conical relief on top surface	−0.222	−0.373	7.80
(m) Custom contoured insole with 6 x tissue stiffness, 14mm diameter cylindrical relief, & constrained tissue movement	−0.167	−0.252	13.51
(n) Custom contoured insole with 2.5 x tissue stiffness, 14mm diameter cylindrical relief, & constrained tissue movement	−0.171	−0.249	14.47
(o) Custom contoured insole with 6 x tissue stiffness, 20mm diameter cylindrical relief, & constrained tissue movement	−0.172	−0.256	14.06
(p) Custom contoured insole with 6 x tissue stiffness, 25mm base diameter 2.5mm deep conical relief on top surface, & constrained tissue movement	−0.168	−0.254	13.52
(q) Custom contoured insole with 6 x tissue stiffness, 25mm base diameter 3 mm deep conical relief on bottom surface, & constrained tissue movement	−0.169	−0.254	13.69
(r) Custom contoured insole with 2.5 x tissue stiffness, 25mm base diameter 3 mm deep conical relief on bottom surface, & constrained tissue movement	−0.170	−0.250	14.36

Table 4. Optimization of Pedorthic Treatment for Vertical Calcaneal Osteophyte
Stresses–Strains in Heel Pad Soft Tissue vs Pedorthic Insole Stiffness & Geometry

Pedorthic Insole	Heel Pad Maximum Cauchy Stress (MPa)	Heel Pad Maximum Green Strain (mm/mm)	Heel Pad Maximum Strain Energy Density ($x10^{-3}$ Joule / mm^3)
(a) No Insole	−6.538	−0.497	822.9
(b) Standard flat insole with 1x stiffness of heel pad tissue	−5.160	−0.4916	529.0
(c) Standard flat insole with 2.5 x stiffness of heel pad tissue	−5.808	−0.495	671.7
(d) Standard flat insole with 6 x stiffness of heel pad tissue	−6.170	−0.496	748.8
(e) Standard flat insole with 6 x tissue stiffness & 25mm base diameter 2.5mm deep conical relief on bottom surface	−4.634	−0.486	430.2
(f) Standard flat insole with 6 x tissue stiffness & 25mm base diameter 2.5mm deep conical relief on top surface	−4.544	−0.486	415.0
(g) Standard flat insole with 6 x tissue stiffness & 20mm diameter cylindrical relief	−2.796	−0.458	216.5
(h) Standard flat insole with 6 x tissue stiffness & 14mm diameter cylindrical relief	−4.563	−0.485	423.8
(i) Custom contoured insole with 6 x tissue stiffness & 14mm diameter cylindrical relief	−2.270	−0.445	160.1
(j) Custom contoured insole with 2.5 x tissue stiffness & 14mm diameter cylindrical relief	−2.186	−0.440	152.8
(k) Custom contoured insole with 6 x tissue stiffness, 20mm diameter cylindrical relief	−1.470	−0.3972	72.3
(l) Custom contoured insole with 6 x tissue stiffness, 25mm base diameter 2.5mm deep conical relief on top surface	−1.946	−0.4353	119.5
(m) Custom contoured insole with 6 x tissue stiffness, 14mm diameter cylindrical relief, & constrained tissue movement	−0.351	−0.252	13.4
(n) Custom contoured insole with 2.5 x tissue stiffness, 14mm diameter cylindrical relief, & constrained tissue movement	−0.318	−0.249	14.5
(o) Custom contoured insole with 6 x tissue stiffness, 20mm diameter cylindrical relief, & constrained tissue movement	−0.184	−0.256	14.0
(p) Custom contoured insole with 6 x tissue stiffness, 25mm base diameter 2.5mm deep conical relief on top surface, & constrained tissue movement	−0.317	−0.254	13.5
(q) Custom contoured insole with 6 x tissue stiffness, 25mm base diameter 3mm deep conical relief on bottom surface, & constrained tissue movement	−0.304	−0.254	13.7
(r) Custom contoured insole with 2.5 x tissue stiffness, 25mm base diameter 3mm deep conical relief on bottom surface, & constrained tissue movement	−0.391	−0.264	14.3